AD-A034 119 JOHNS HOPKINS UNIV BALTIMORE MD F/G 8/8
LECTURES ON ESTUARINE CIRCULATIONS AND MASS DISTRIBUTIONS.(U)
DEC 76 R R LONG
UNCLASSIFIED TR-9-SER-C NL

1 OF 2
ADA034119

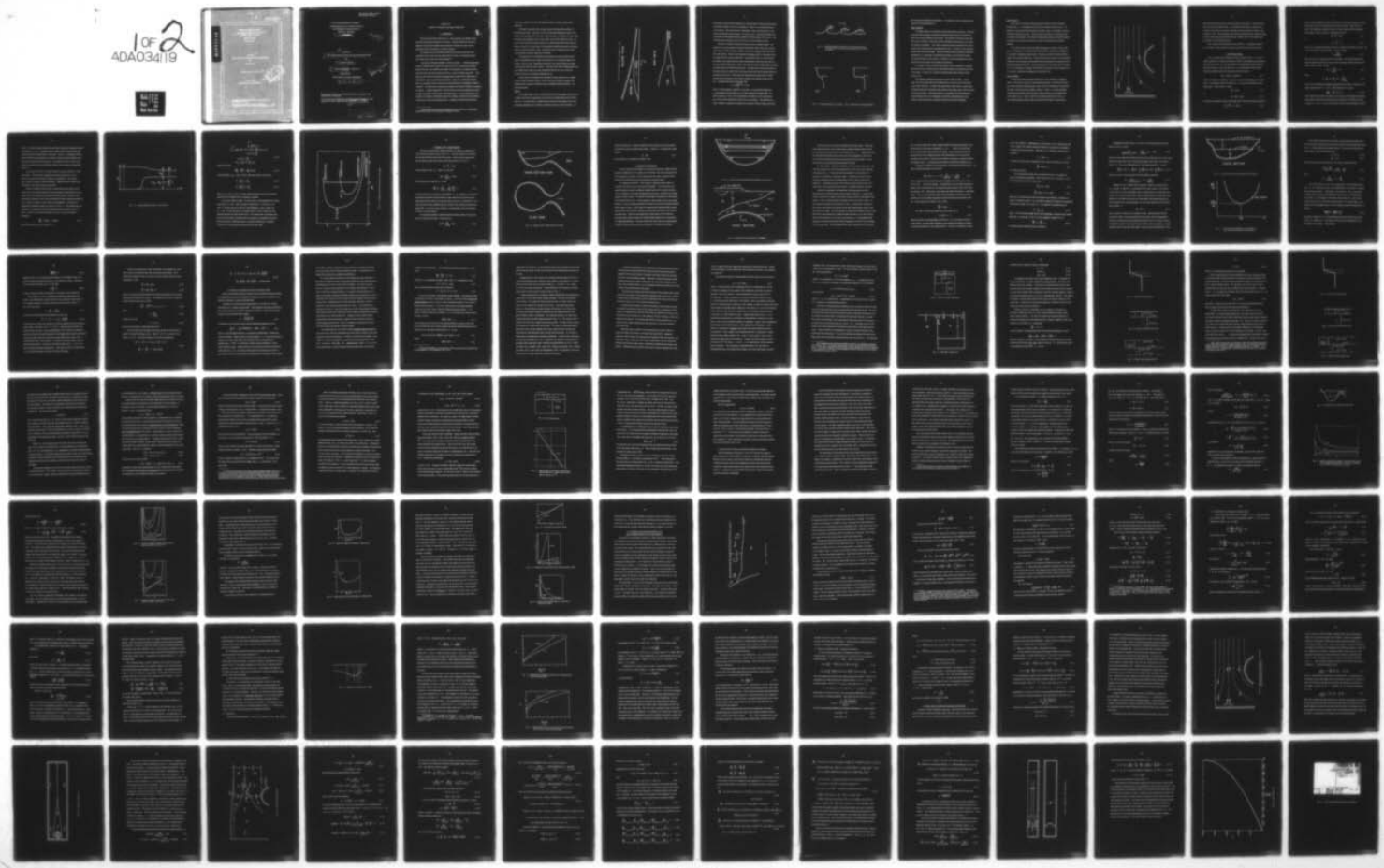

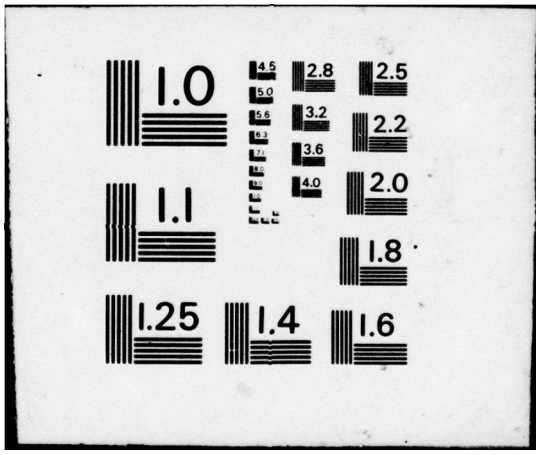
1.0
1.1
1.25
1.4
1.6
1.8
2.0
2.2
2.5
2.8
3.2
3.6
4.0
4.5
5.0
5.6

THE JOHNS HOPKINS UNIVERSITY

Departments of Earth & Planetary Sciences
and Mechanics & Materials Science
Baltimore, Maryland

(11) Dec[redacted]76

(12) 99 P.

(6)

Lectures on
ESTUARINE CIRCULATIONS AND MASS DISTRIBUTIONS

By

(10) Robert R. Long

(9) Technical Report No. 9 (Series C)

Sponsored By

THE OFFICE OF NAVAL RESEARCH

(14) TR-9-Ser-C

This research was supported by the Office of Naval Research, Fluid Dynamics Division, under Contract No. N00014-75-C-0805

(15)

191750

Lectures on

Estuarine Circulations and Mass Distributions

1. Introduction

These lectures concern estuaries or, more precisely, my special recent interests in the physical aspects of estuaries. Donald Pritchard at The Johns Hopkins University has studied these systems for twenty-five years and has attempted (1967) to formulate a workable definition:

"An estuary is a semi-enclosed coastal body of water which has a free connection with the open sea and within which sea water is measurably diluted with fresh water derived from land drainage."

I can quarrel with this definition in certain respects. Pritchard apparently wanted a definition which required an estuary to have an "estuarine circulation" characterized by water outflow in the upper layercomposed of a mixture of fresh water and salt water and an inflow in the lower layers of saltier sea water[1] . The presence of this kind of circulation distinguishes an estuary from other types of embayments and is a useful characterization. However, as Pritchard himself states, it excludes a body of water such as the Baltic Sea by including the adjective "coastal". The Baltic has an estuarine circulation and I think it should be considered an estuary. A further objection is to the last four words in the definition which put an undue importance on the source of the fresh water. It may be interesting, for example, to consider a theoretical model of an estuary in which the direct addition of rain water may be an important source. Certainly we should not exclude the

---

[1] In the typical estuary density differences due to salinity are considerably greater than those due to temperature (Pritchard, 1965).

fresh water addition from the rain falling directly on a body as large as the Baltic Sea.

Pritchard's definition of an estuary requires an appreciable amount of incoming fresh water. However, we will see that interesting three-layer circulations with resemblances to two-layer estuarine-type circulations can occur when the fresh-water supply is zero or very small, and we will include this case. We may even go further and include situations in which evaporation exceeds precipitation and run-off. In such cases, for example the Mediterranean Sea and Laguna Madre in Texas (Pritchard, 1965), inverse two-layer circulations exist which also resemble the classic estuarine circulation.

Pritchard goes on to distinguish several types of estuaries based on geological considerations of the origin of the estuaries, for example drowned river valleys, which he calls "coastal plain estuaries" and coastal indentures gouged out by glaciers which he calls "fjords". Certainly fjords differ fundamentally from such coastal plain estuaries as the Chesapeake Bay but the way in which the estuaries formed is not directly important for us.

It will clarify our problem if we attempt to classify estuaries in a manner similar to that of Stommel (1951), based in part on the relative strength of the turbulence that causes the mixing of waters of different salinity (density). We define four types:

Type 1:

The simplest type is one in which the fresh water flows gently out to sea over a wedge of salt water originating in the sea with no mixing between the two fluids (Fig. 1.1). The fresh water is lighter than the salt water and tends to over-ride, ultimately spreading out in a thinner and thinner layer as it moves seaward. In

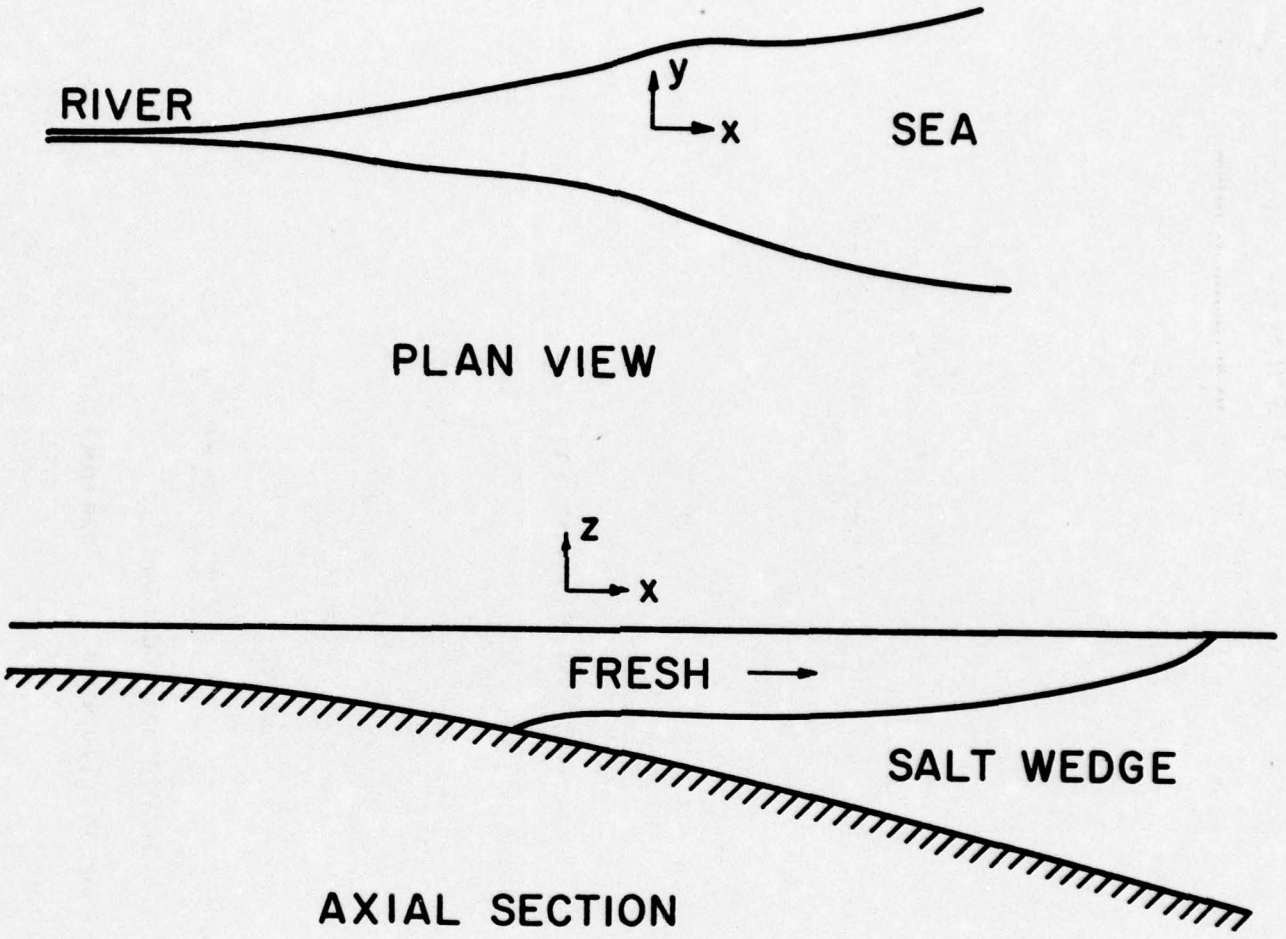

Fig. 1.1 Mouth of a river emptying into the ocean.

the absence of any mixing the upper layer remains fresh and the mass flux across any section is equal to the river discharge R. There is a zero salt flux across every section. Since the interface is stationary, if the lower fluid may be considered frictionless and barotropic, it will be at rest. Among other things, this means that the horizontal pressure gradient in the lower layer will be zero. The salt wedge may penetrate up the river 50 km or more (Pritchard, 1965).

Of course, frictional effects and mixing are never entirely absent. For example even in the absence of wind and tide the flow of the river water over the salt wedge will tend to produce unstable waves at the interface which will break and cause mixing. This has been studied by Keulegan (1949) in a laboratory flow of a light fluid over heavier salty fluid. As pictured in Fig. 1.2, waves formed and eddies were ejected from the crests causing some of the lower salt water to be mixed with the upper fluid. In the river this will cause the upper fluid to become somewhat salty as it flows toward the sea. The salty water comes from below so that there must be a (small) flow in the lower layer from the sea up the estuary to replenish the lost salt. In this kind of mixing none of the upper fluid is mixed into the lower fluid and the lower water remains of the density of water in the sea. Keulegan found that mixing began when

$$\theta = \left(\nu g \frac{\Delta\rho}{\rho_f}\right)^{\frac{1}{3}} / \bar{u} = 0.178$$

where ν is the kinematic viscosity, g is gravity, $\Delta\rho$ is the density difference, ρ_f is the density of fresh water and $\bar{u}$ is the velocity of the upper fluid. For typical values in a river, this corresponds to velocities of a few centimeters per second so that instabilities of this kind are very likely. The definition of a Type 1 estuary is restricted to situations in which the (weak) mixing is primarily

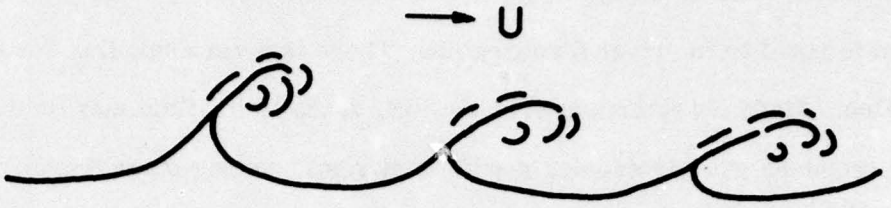

Fig. 1.2 Breaking waves at interface of a two fluid experiment. The lower fluid is at rest and the upper fluid is moving at speed U.

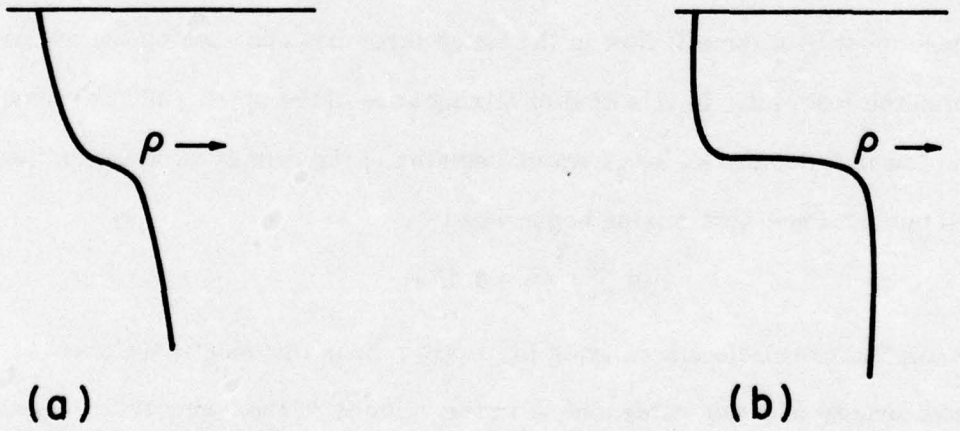

Fig. 1.3 Density profiles in an estuary. Fig. 1.3b portrays a sharp halocline.

due to the wave breaking at the interface. An example of a Type 1 estuary is the mouth of the Mississippi River.

Type 2 Estuary.

Two other effects are important in producing mixing in estuaries. The first is the tide which produces motions and breaking internal waves in the fluid and these in turn cause turbulence and mixing. The second is the stress of the wind. This causes velocities in the water and the resulting vertical shears are a source for energy of turbulence. The result is increased mixing compared to the Type 1 estuary and a density profile resembling that in Fig. 1.3a with a fairly continuous density distribution with height. Here the density increases gradually with depth although there is frequently an identifiable halocline across which the density increase with depth is more marked. Examples are the Chesapeake Bay and the mouth of the James River which empties into the bay.

We include in Type 2 the fjord-type estuary which is typically so deep that the lower layers are relatively inert with little mixing and a density equal to that of sea water. In this case a relatively sharp halocline often exists as shown in Fig. 1.3b.

The mixing is typically much larger in Type 2 than in Type 1. In the Type 1 the flux of salt water into the upper layer is less than or at most of the order of the river flow. In Type 2 the upward flux of salty water is much larger so that the total flow of brackish water seaward in the upper layers will be several times the river flow. In the James River, for example, the total discharge is some twenty times the river discharge so that the compensating flow up the estuary in the lower layers is nineteen times the fresh water discharge.

Type 3 Estuary.

If the source of mixing is strong enough the estuary may be sectionally homogeneous, i.e., thoroughly mixed from top to bottom and side to side. Although the vertical and lateral gradients of salinity vanish, a horizontal, seaward variation of salinity may exist. In the idealized case there is no estuarine type circulation in the estuary. The observed longitudinal gradient of salinity requires a transfer of salt up the estuary and this must be accomplished by turbulent diffusion.

It is possible that strictly sectionally homogeneous estuaries do not really exist. For example, the estuary of the Mersey River in England was thought to be vertically homogeneous until Bowden, Fairbairn and Hughes (1959) reported a slight vertical salinity difference. This raises the basic question as to the relative importance of the advective salt flux $\bar{u}\bar{S}$ set up by the estuarine circulation and the turbulent longitudinal flux $\overline{u'S'}$. In these expressions u is velocity and S is salinity. If $\bar{u} = 0$, the estuarine circulation is absent but, because $\bar{S}$ is large compared to S', a very weak circulation can transport a great deal of salt.

Type 4 Estuary.

In this estuary the fresh-water influx from river discharge is negligibly small. If the water in the sea is of homogeneous density, it will fill the estuary and, since no density variations exist, there will be no gravitational circulations. The Type 4 estuary can have motions, however, if there is a vertical gradient of density in the outside water and if the mixing is greater in the estuary than in the outside water. Then we will have the situation portrayed in Fig. 1.4. The constant density surfaces slope as shown and this leads to accelerations

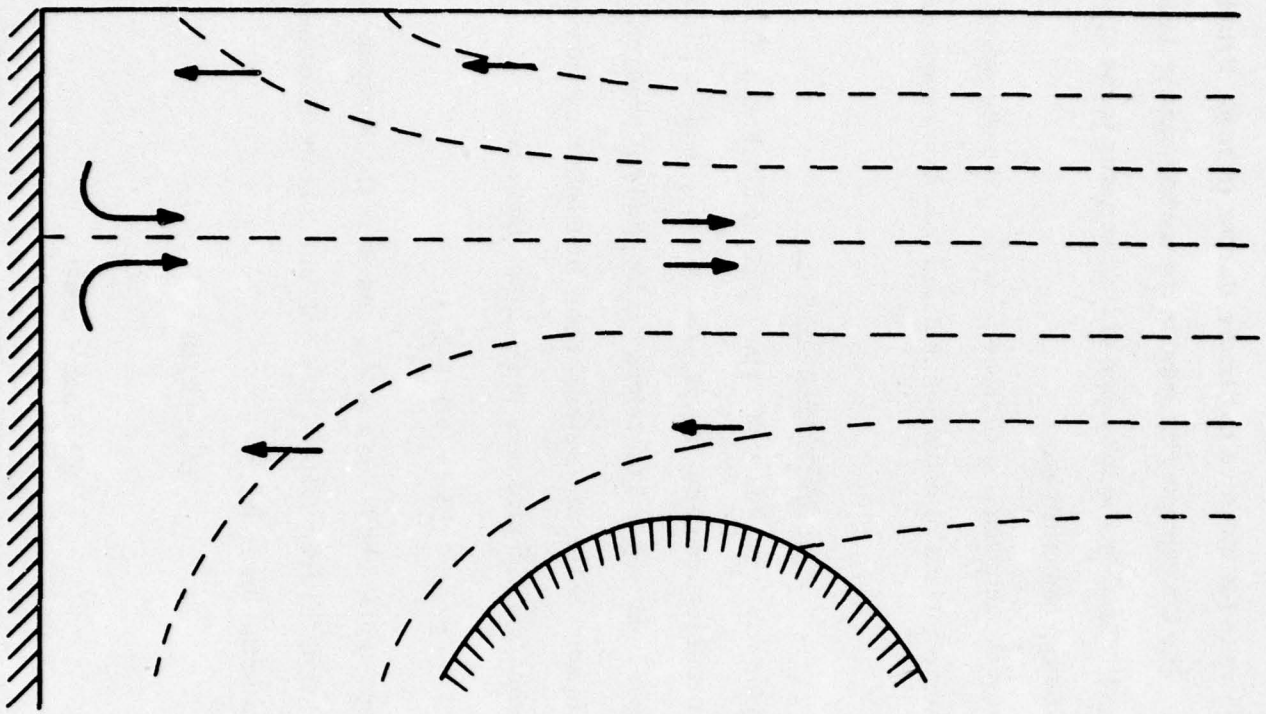

Fig. 1.4 Schematic density distribution in a Type 4 estuary.

which produce the three-layer circulation pictured in the figure. This possibility was first raised by Hachey (1934). A circulation of this kind was inferred from a study of acid wastes in the water in Baltimore Harbor (Stroup, Pritchard, and Carpenter, 1961). The Chesapeake Bay outside the harbor has the required density variation with height caused by the presence of lighter water in the upper layers originating in the Susquehanna River.

This concludes the introduction to these lectures. In subsequent sections we will consider some aspects of estuaries in detail based on recent research.

2. Salt-Wedge Estuary

Let us consider first an estuary of Type 1 pictured in Fig. 1.1. We will confine attention to an idealized situation in which we may neglect mixing entirely. Then the lower layer is at rest and therefore the longitudinal pressure gradient along the estuary is zero in the salt water. From hydrostatics (and using the Boussinesq approximation) the pressure in the lower layer is

$$p/\rho_f = g(H-z) + \Delta b(H-h-z) \tag{2.1}$$

where b is buoyancy, defined by $b = g(\rho-\rho_f)/\rho_f$ and Δb is the buoyancy of the salt water. The equation of the free surface is $z = H$, and h is the thickness of the upper layer. Thus in the lower layer

$$gH_x = h_x \Delta b \tag{2.2}$$

or

$$gH = h\Delta b + \text{const} \tag{2.3}$$

We assume irrotational motion in the upper layer so that the Bernouilli equation is

$$\frac{p}{\rho_f} + \frac{u^2}{2} + gz = \text{const} \tag{2.4}$$

where u is the longitudinal velocity which will be nearly uniform across a section. We neglect the other two components of the kinetic energy. They will be very small if the length scale along the estuary is large compared with the depth and if the change of width is gradual. Hydrostatics leads to

$$gH + \frac{u^2}{2} = \text{const} \tag{2.5}$$

or

$$h\left(1 + \frac{F^2}{2}\right) = E \tag{2.6}$$

where E is a constant proportional to the sum of kinetic and potential energies, and F is the densimetric Froude number. It may be written

$$F^2 = \frac{R^2}{W^2 h^3 \Delta b} \tag{2.7}$$

where R is the river discharge and W is the width. Let us non-dimensionalize using the depth of the fluid h_o at the tip of the salt wedge and the width W_o of the estuary at this section. We have

$$2h' + \frac{F_o^2}{(h'W')^2} = E' \tag{2.8}$$

where

$$h' = \frac{h}{h_o}, \quad W' = \frac{W}{W_o}, \quad F_o^2 = \frac{R^2}{W_o^2 h_o^3 \Delta b} \tag{2.9}$$

and E' is non-dimensional constant proportional to the energy. If energy is conserved along the flow $E' = 2 + F_o^2$. Differentiating (2.8), we get

$$\frac{dh'}{dW'} = \frac{h'}{W'} F^2/(1-F^2) \tag{2.10}$$

This shows that the depth of the upper level decreases with distance downstream (assuming the width increases downstream) if and only if conditions are supercritical, i.e., $F^2 > 1$. Eq. (2.6) shows that F^2 then increases along the estuary.

Thus, if we require energy conservation and that h decreases everywhere toward the mouth, $F_o^2 \geq 1$, i.e. conditions must be supercritical at the top of the salt wedge and therefore supercritical everywhere. In fact, it is physically obvious that h must decrease ultimately as we proceed seaward so that conditions must ultimately be supercritical in any case. It is possible, however, that h could increase near the tip for some distance so that we may consider the possibility that $F_o^2 < 1$.

We see from (2.6) and (2.10) that h begins to increase and that F^2 begins to decrease. These behaviors continue toward the mouth and h can never decrease as required ultimately by physical considerations. We conclude that if energy is conserved along the estuary, conditions must be supercritical everywhere and h must decrease montonically.

Another possibility exists however, namely that the flow starts out subcritical with h increasing downstream and then changes discontinuously at some section (with loss of energy in an internal hydraulic jump) to a smaller h and supercritical conditions, with h then decreasing with farther distance downstream. To see if this is possible we must make two investigations. In the first we calculate the momentum balance in a jump as in Fig. 2.1. We consider the rate of change of x-momentum of the fluid contained between Sections A and B at time t. At time dt it is between sections A' and B'. Its rate of change of momentum,

$$\frac{dM}{dt} = u_b^2 W h_b \rho_f - u_a^2 W h_a \rho_f \qquad (2.11)$$

equals the pressure forces on the fluid, i.e.,

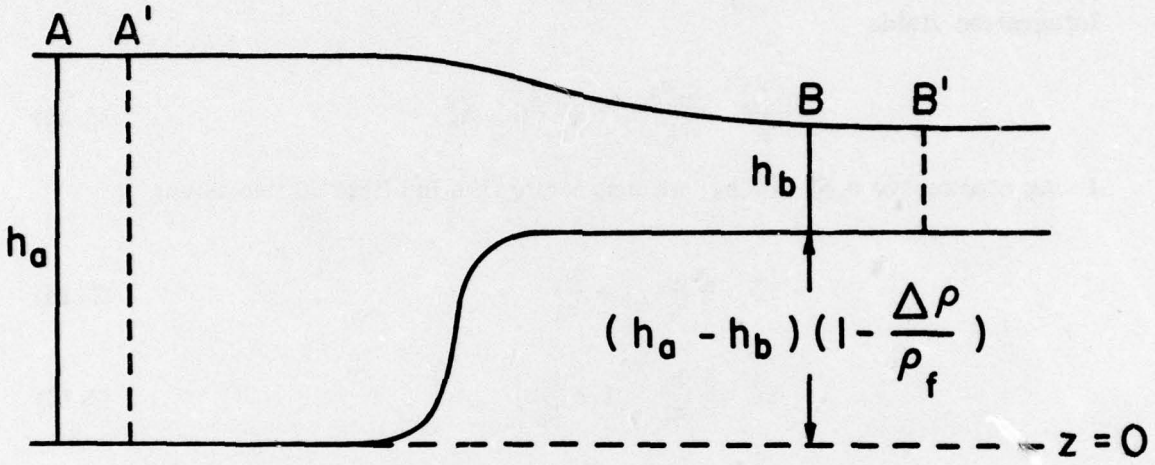

Fig. 2.1 Internal hydraulic jump in a salt wedge.

$$W\int_0^{h_a} \rho_f g(h_a - z)dz - W\int_{(h_a-h_b)\left(1-\frac{\Delta\rho}{\rho_f}\right)}^{h_a - \frac{\Delta\rho}{\rho_f}(h_a-h_b)} \rho_f g\left[h_a - \frac{\Delta\rho}{\rho_f}(h_a-h_b) - z\right]dz$$

$$-W\int_0^{(h_a-h_b)\left(1-\frac{\Delta\rho}{\rho_f}\right)} \rho_f g\left[h_a - (1+\frac{\Delta\rho}{\rho_f})z\right]dz \qquad (2.12)$$

Integration yields

$$\frac{u_b^2 h_b}{g} - \frac{u_a^2 h_a}{g} = \frac{\Delta\rho}{2\rho_f}(h_a^2 - h_b^2) \qquad (2.13)$$

Using continuity, $u_a h_a = u_b h_b$ we may write this in either of two ways:

$$F_a^2 = \frac{1}{2}\frac{h_b}{h_a}\left(1 + \frac{h_b}{h_a}\right) \qquad (2.14)$$

$$F_b^2 = \frac{1}{2}\left(\frac{h_a}{h_b}\right)^2\left(1 + \frac{h_b}{h_a}\right) \qquad (2.15)$$

Since $h_b \leq h_a$, $F_a^2 \leq 1$, $F_b^2 \geq 1$ so that a jump downstream from sub-critical to supercritical is possible from a momentum viewpoint.

Let us now consider energy. We may choose a representative sub-critical initial flow $F_o^2 = 0.25$. Then if energy is conserved $E' = 2.25$ in Eq. (2.8). Fig. 2.2 contains this curve plus one corresponding to a lower energy level $E' = 1.50$. We see that there is a possible jump to a lower energy from the subcritical branch as shown by the arrow. We conclude that a subcritical flow at the tip of the wedge is possible with h increasing very gradually initially but there must then be a hydraulic jump to a smaller h followed by a monotonic reduction of h as the upper fluid spreads out over the wedge.

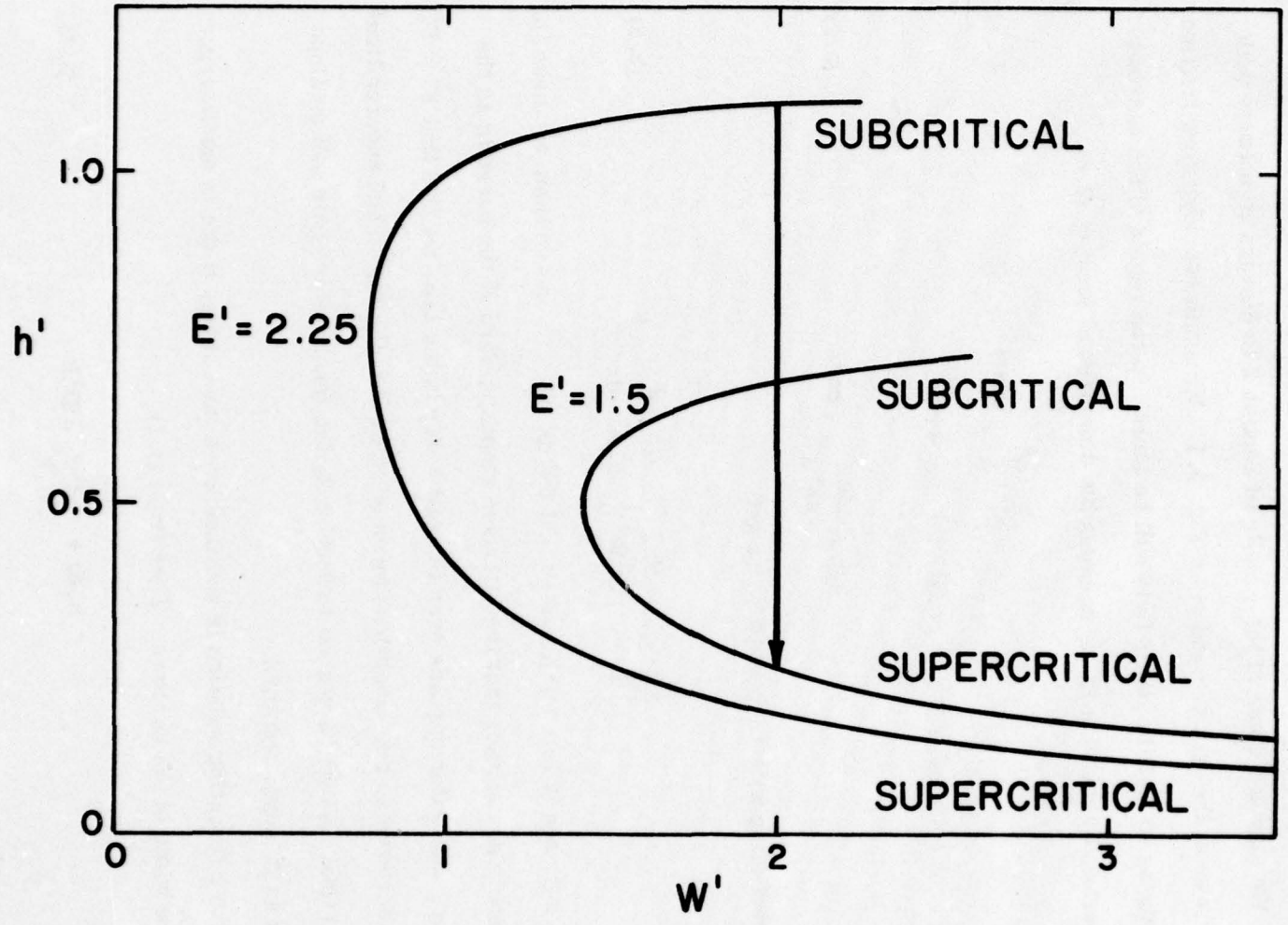

Fig. 2.2 Energy curves for flow above a salt wedge.

3. Estuary with a Control Section.

We may use some of the results of Section 2 to discuss an estuary with a narrows at the seaward end as in Fig. 3.1. We again consider zero friction and mixing so that the lower fluid will be inert. In the region of the narrows the Bernouilli equation is the same as the dimensional form of (2.6),

$$h\Delta b + \frac{u^2}{2} = \text{const} \tag{3.1}$$

Using continuity $uhW = q_1 = \text{const}$, we may write

$$h\Delta b + \frac{q_1^2}{2h^2W^2} = \text{const} \tag{3.2}$$

Differentiating with respect to x, we get

$$\frac{dh}{dx}\left[\Delta b - \frac{q_1^2}{h^3W^2}\right] - \frac{q_1^2}{h^2W^3}\frac{dW}{dx} = 0 \tag{3.3}$$

At the narrows W is a minimum so that $dW/dx = 0$. If, in addition, we make the reasonable assumption that the interface slopes upward at the narrows as the issuing fresh water spreads over the salt water in the sea, we find that $F^2 = F_c^2 = 1$ at the narrows so that conditions become critical at the mouth and supercritical beyond this. As we have seen in Section 2, the fresh-water layer will continue to thin as it moves seaward.

An interesting relation is obtained when the estuary width is much larger than the width of the narrows. Then from (3.2)

$$h_c\Delta b + \frac{q_1^2}{2W_c^2h_c^2} = D\Delta b \tag{3.4}$$

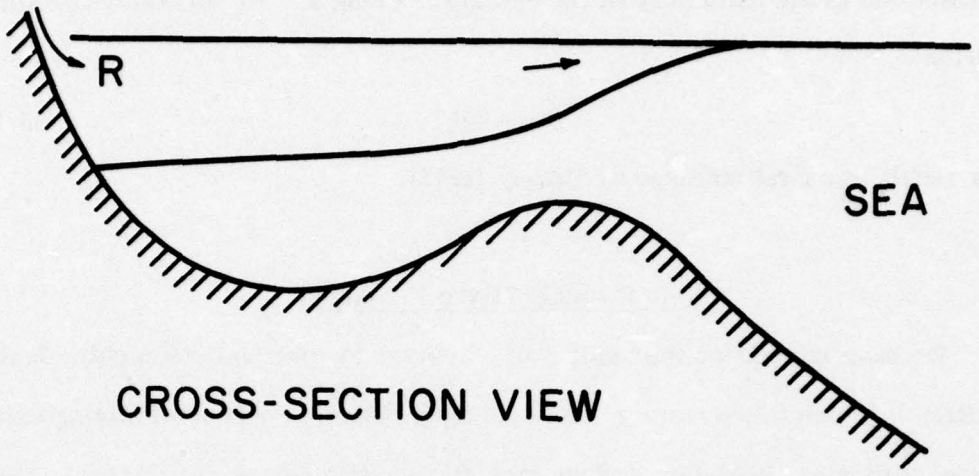

CROSS-SECTION VIEW

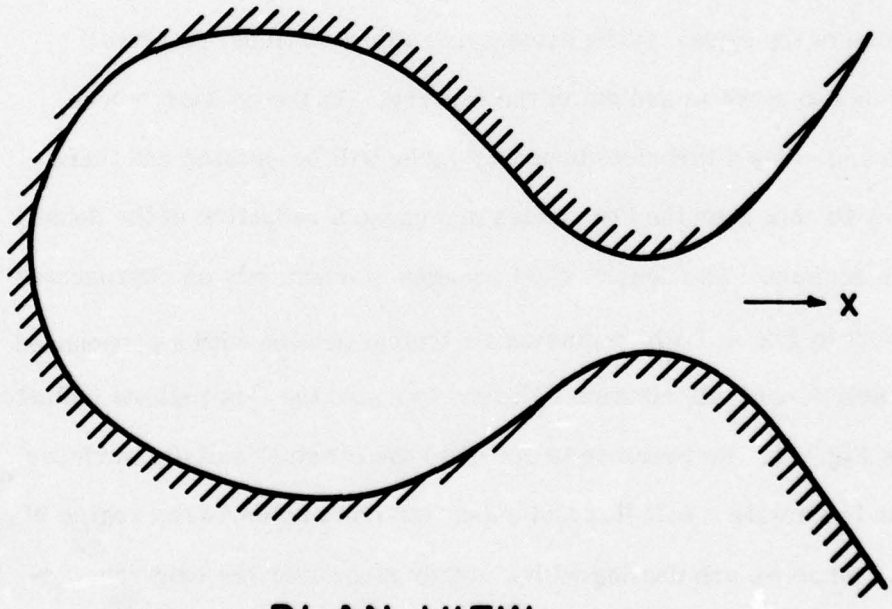

PLAN VIEW

Fig. 3.1 Estuary with a constriction or narrows.

where the subscript "c" denotes conditions at the narrows and D is the depth of the halocline in the main body of the estuary. Using $F_c^2 = 1$ we obtain the simple relation

$$h_c = \tfrac{2}{3}D \qquad (3.5)$$

This result was first obtained by Binney (1972).

4. Strongly Mixed Estuaries

We have introduced the subject of estuaries by discussing a highly idealized situation in which there is no mixing (and no friction). Sources of mixing exist in all real estuaries, however, and we may discuss two causes in addition to the tendency for breaking waves on the halocline as described above.

(1) Influence of the tides. If the estuary is subject to tides, these will cause tidal currents to move in and out of the estuary. As the current moves along the bottom and sides a turbulent boundary layer will be created and there will be a tendency to mix near the boundaries and cause a reduction of the density gradient in those regions. The density field changes momentarily as represented by the dashed lines in Fig. 4.1 which portrays a typical pattern with a pronounced halocline. The new density distribution will tend to cause the flow pattern indicated by the arrows in Fig. 4.1. The result is to separate the constant salinity surfaces in the interior and to create a salt flux and mass flux from below to the region of the upper layer. Since we are dealing with a steady state over the long run, processes must exist to restore the original density gradient and, in particular, to maintain the halocline. The loss of salt in the lower layers is compensated by an influx of salt from the sea due to the estuarine circulation that develops.

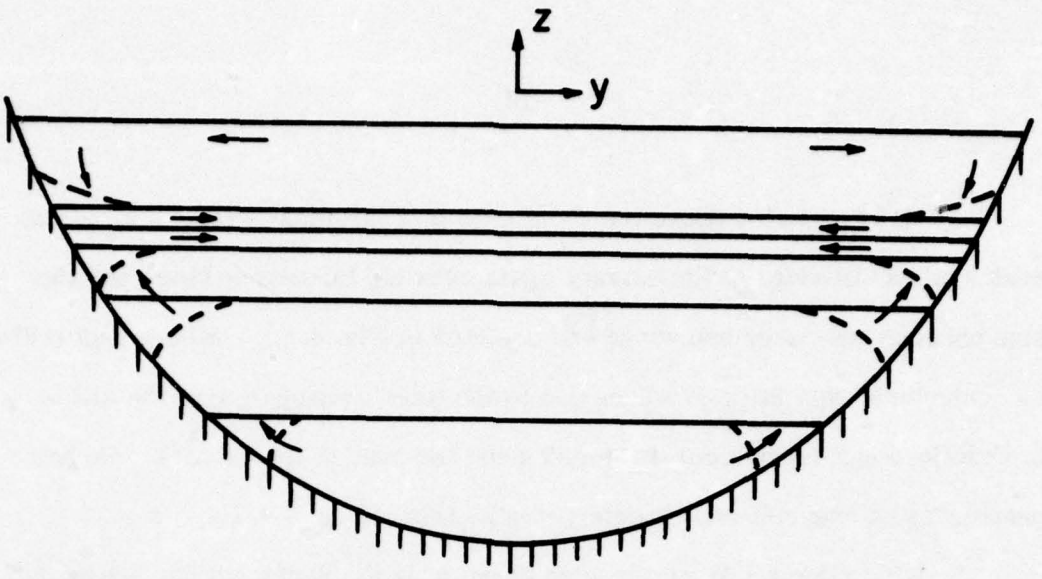

Fig. 4.1 Effects of mixing along sides and bottom of an estuary.

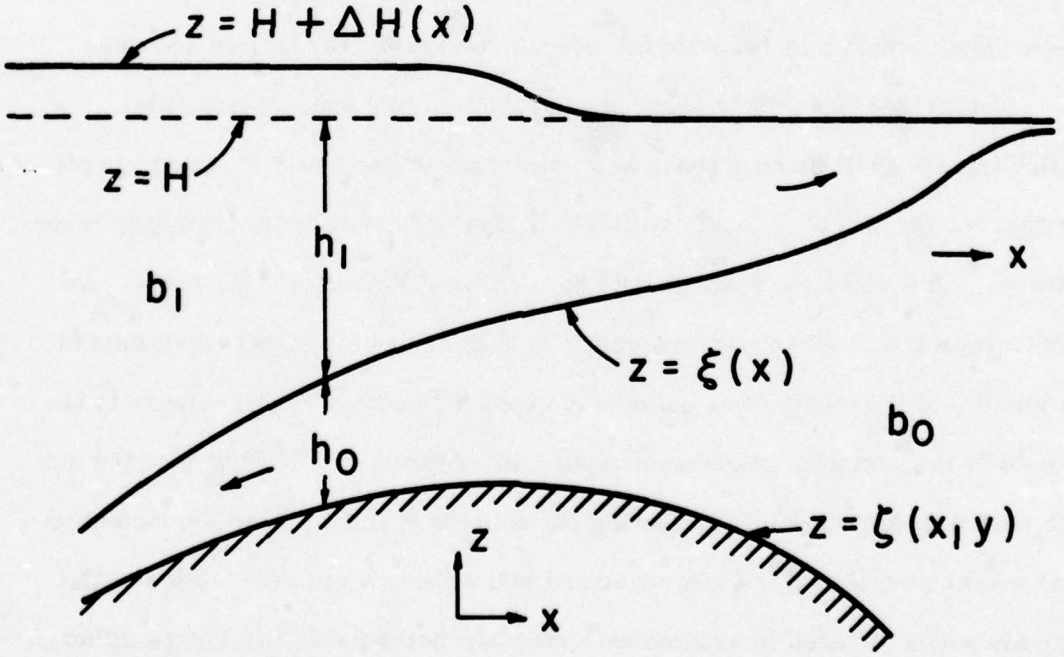

AXIAL SECTION

Fig. 4.2 Conditions near the mouth of an estuary.

The tides will also cause the development of internal waves. These may break against the sides of the estuary again creating turbulence there and the same phenomenon described above and depicted in Fig. 4.1. Stigebrandt (1976) has conjectured that internal waves due to the tides propagate over the sill of the Oslofjord and break against the sides and the head of the estuary. He has constructed an experiment that demonstrates this effect.

(2) Wind effects. When the wind blows over the surface of the water, the resultant agitation, for example breaking surface waves, will cause turbulence in the upper levels. To the extent that this penetrates to lower layers, for example to the halocline, mixing will result. In addition the wind will cause currents in the water and the resulting shear will be a source of energy for turbulence. In addition the stress of the wind may cause internal waves in the deeper layer which may break in the interior or against the bottom and sides.

Obviously a quantitative representation of mixing processes will be difficult and we will discuss these at some length in Section 5. A great simplification results if the mixing is sufficiently strong to produce a thoroughly mixed estuary. This was first discussed by Stommel and Farmer (1952, 1953). We may discuss the problem with reference to Fig. 4.2 which shows conditions in the vicinity of the mouth of an estuary (on the left) connecting the estuary to the open sea (on the right). We have assumed an estuarine circulation near the mouth with fluid of mean buoyancy b_1 flowing out with mass flux q_1 over the incoming fluid with the buyancy b_0 of sea water and mass flux q_0. In this portion of the analysis we do not need to assume uniform buoyancies in the two layers although we will do this later. The mean depth of the water averaged across the channel

is $\bar{h}$, the mean width is $\bar{W}$. Other lengths required to specify the geometry of the estuary and its mouth may be denoted by $L_1, L_2, \ldots$. There is a fresh-water flux R into the estuary and some kind of mixing. In the present discussion the precise nature of the mixing processes is not important (as we will see) but to be definite and simple we will assume the mixing is caused by a rotating propellor with angular speed ω. Its geometry and location are specified by lengths $a_1, a_2, \ldots$.

A quantity of importance in the discussion is the buoyancy difference $b_0 - b_1 = \Delta b$. From dimensional analysis we may write

$$\frac{\Delta b}{b_0} = f_1(Q_f, \Omega, \ldots), \quad Q_f = \frac{R}{b_0^{\frac{1}{2}} \bar{h}^{\frac{3}{2}} \bar{W}}, \quad \Omega = \frac{\omega a_1}{(\bar{h} b_0)^{\frac{1}{2}}} \tag{4.1}$$

where a number of non-dimensional ratios of lengths of the form $L_1/\bar{h}$, $L_2/\bar{h}, \ldots$, $a_1/\bar{h}$, $a_2/\bar{h}, \ldots$ have been omitted. Certainly $\Delta b/b_0$ will vary with the quantity Ω; indeed $\Delta b/b_0$ will decrease as Ω increases from the maximum value of one when the mixing is zero. Ultimately, if the estuary has finite dimensions, a sufficiently large Ω, say Ω_m, will cause the estuary to be thoroughly mixed and any further increase of Ω will not further decrease Δb and it will assume its minimum value Δb_m. Since $\partial(\Delta b/b_0)/\partial\Omega$ when $\Delta b = \Delta b_m$, we get

$$\frac{\Delta b_m}{b_0} = f_2(Q_f, \ldots) \tag{4.2}$$

The ratio η of the mean depth of the lower layer to $\bar{h}$ is

$$\eta = f_3(Q_f, \Omega, \ldots) \tag{4.3}$$

When the estuary is just thoroughly mixed and $\Delta b = \Delta b_m$, any further increase in the mixing Ω can only affect conditions at the mouth by the tendency to further increase the turbulence in the outflowing fluid. This effect is difficult to analyse

and we will neglect it. Subsequently we will assume, in fact, perfect fluid flow in the vicinity of the mouth so that the turbulence is assumed to be negligible compared to the mean motions. Then for $\Omega \geq \Omega_m$, η assumes a fixed value η_m such that

$$\eta_m = f_4(Q_f, \dots) \tag{4.4}$$

In general we notice that a combination of (4.1) and (4.3) permits us to write

$$\frac{\Delta b}{b_o} = f_5(Q_f, \eta, \dots) \tag{4.5}$$

for arbitrary mixing.

Let us attempt to find the form of the function in Eq. (4.5) subject to several simplifying assumptions. With reference to Fig. 4.2 and Fig. 4.3 the Bernoulli equations in the two layers are

$$\frac{u_1^2}{2} + g\Delta H = \text{const} \tag{4.6}$$

$$\frac{u_0^2}{2} + g\Delta H - h_1 \Delta b = \text{const} \tag{4.7}$$

where h_1 is the distance from the free surface to the interface, and where we assume irrotational motion. Let us justify the neglect of the other two components of the kinetic energy in (4.6) and (4.7). The equation of continuity leads to

$$\frac{u}{\lambda} \sim \frac{v}{\bar{W}} \sim \frac{w}{\bar{h}} \tag{4.8}$$

where λ, $\bar{W}$ and $\bar{h}$ denote length scales in the longitudinal, transverse and vertical directions. In each layer v^2 and w^2 will be negligible compared to u^2 if

$$\frac{\bar{W}^2}{\lambda^2} \ll 1 \quad \frac{\bar{h}^2}{\lambda^2} \ll 1 \tag{4.9}$$

We assume that the channel has these properties.

Eliminating ΔH between Eqs. (4.6) and (4.7) and introducing the constant fluxes q_1 and q_0, we have

$$\frac{q_0^2}{2\Delta b B_0^2 [H-h_1-\bar{\zeta}(x)]^2} - \frac{q_1^2}{2\Delta b \bar{B}_1^2 h_1^2} - h_1 = \text{const} \qquad (4.10)$$

where B_0 is the width of the channel at the level of the interface, $\bar{B}_1$ is the average width in the upper layer and $\bar{\zeta}$ is the average height of the bottom of the channel above $z = 0$. Let us now differentiate Eq. (4.10) with respect to x. We get

$$\frac{dh_1}{dx}(F_0^2 + F_1^2 - 1) = -\frac{d\bar{\zeta}}{dx} F_0^2 + \frac{1}{B_0}\frac{dB_0}{dx}(H-h_1-\bar{\zeta})F_0^2 - \frac{1}{\bar{B}_1}\frac{d\bar{B}_1}{dx} h_1 F_1^2 \qquad (4.11)$$

where F_0 and F_1 are the densimetric Froude numbers defined by

$$F_0^2 = \frac{q_0^2}{\Delta b B_0^2 [H-h_1-\bar{\zeta}]^3}, \quad F_1^2 = \frac{q_1^2}{\Delta b \bar{B}_1^2 h_1^3} \qquad (4.12)$$

Suppose we have a channel with a minimum of width at a certain section (i.e., $dB_0/dx = 0$, $d\bar{B}_1/dx = 0$, presumably at the same section). If the bottom is level there (or if the mean depth is also a minimum there), the left-hand side of Eq. (4.11) is zero at that section. Since we would expect a strong slope of the interface as the upper level moves out of the estuary and spreads laterally and thins vertically in the widening channel, we infer that conditions will be critical at the section, i.e.

$$F_0^2 + F_1^2 = 1 \qquad (4.13)$$

Such a section is referred to as a control section. Experiments by Stommel and Farmer (1953), Assaf and Hecht (1974) and Assaf, Anati and Siegenthaler (1975) have shown that critical conditions do tend to occur in a variety of straits in laboratory models. If the strait is long, friction become important and critical conditions occur at the ends of the strait (Assaf, Anati and Siegenthaler, 1975).

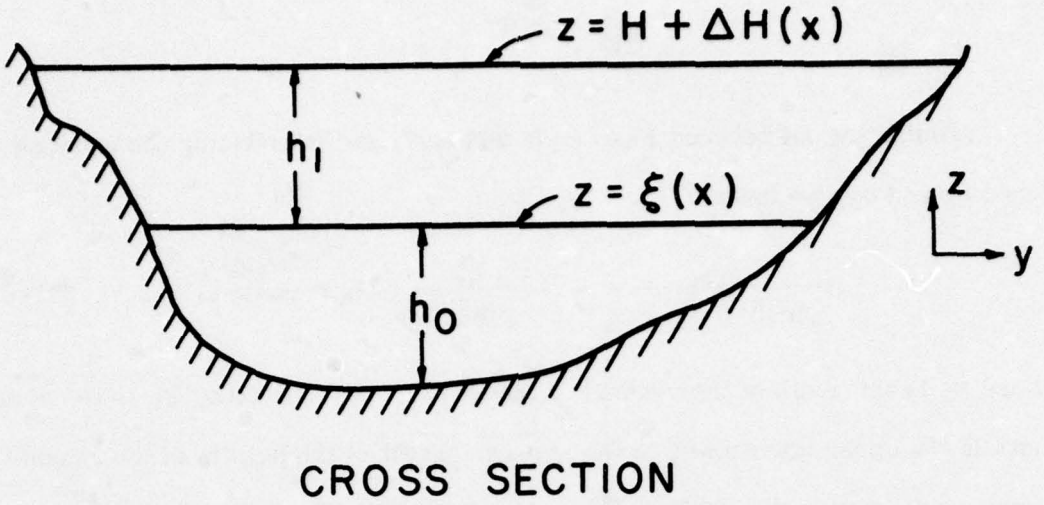

CROSS SECTION

Fig. 4.3 Cross section in the constriction of an estuary.

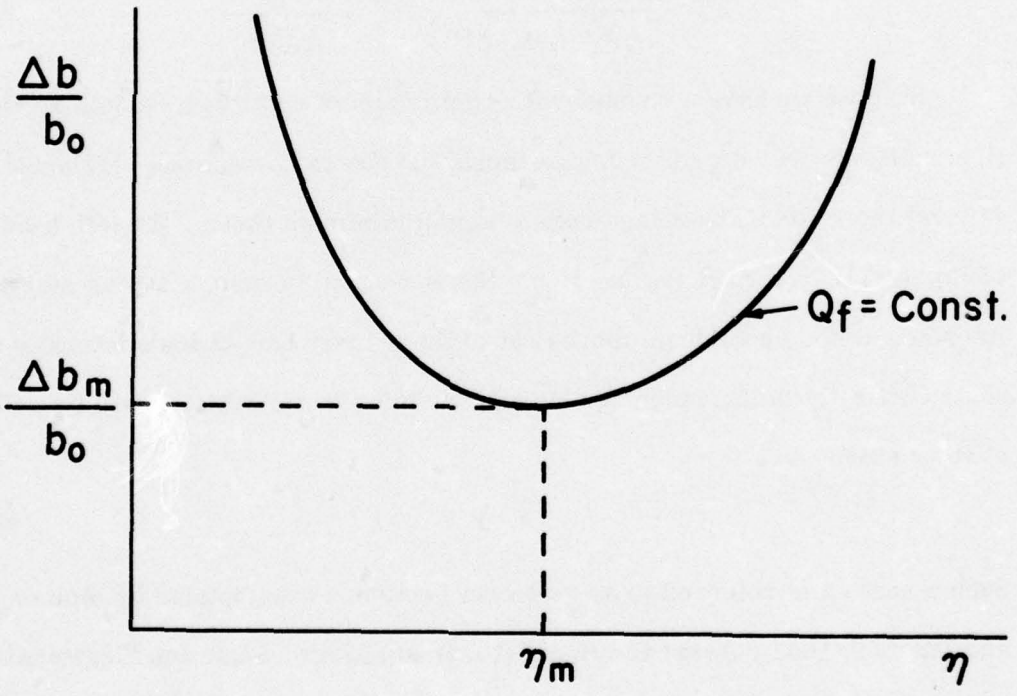

Fig. 4.4 Curve of density difference as a function of non-dimensional thickness of lower layer.

At the control section we let W_o and $\bar{W}_1$ be the values of B_o and $\bar{B}_1$ and η be the ratio of the mean thickness of the lower fluid to the mean depth of the water $(H - \bar{\zeta}) = \bar{h}$ both evaluated at the control section. We also use the equations for conservation of mass and buoyancy (salt)

$$q_o + R = q_1 \tag{4.14}$$

$$q_o b_o = q_1 b_1 \tag{4.15}$$

where R is the fresh water discharge. The critical condition becomes

$$\frac{n^2 Q_f^2 \left(1 - \frac{\Delta b}{b_o}\right)^2}{\eta^3} + \frac{Q_f^2}{(1-\eta)^3} = \left(\frac{\Delta b}{b_o}\right)^3 \tag{4.16}$$

where

$$Q_f^2 = \frac{R^2}{b_o \bar{h}^3 \bar{W}_1^2}, \quad n^2 = \frac{\bar{W}_1^2}{W_o^2} \tag{4.17}$$

For a given value of Q_f, Eq. (4.16) represents a curve like that shown in Fig. 4.4. It is of the form of Eq. (4.5) yielding $\Delta b/b_o$ as a function of η instead of the mixing parameter Ω. Physically, if we increase Ω from a small value, we expect $\Delta b/b_o$ to decrease monotonically from the value 1 corresponding to zero mixing. η will increase or decrease with increase of Ω, and we move on the curve of Fig. 4.4 toward the minimum point. At a certain value Ω_* the estuary will be thoroughly mixed, Δb will no longer decrease and $\partial(\Delta b/b_o)/\partial\Omega = 0$. We have

$$\frac{\partial(\Delta b/b_o)}{\partial \Omega} = \frac{\partial(\Delta b/b_o)}{\partial \eta} \frac{\partial \eta}{\partial \Omega} \tag{4.18}$$

Obviously if $\partial(\Delta b/b_o)/\partial\eta = 0$, corresponding to the minimum point of the curve in Fig. 4.4, $\partial(\Delta b/b_o)/\partial\Omega = 0$ and $\Delta b/b_o$ will have the value appropriate to the thoroughly mixed estuary. The condition

$$\frac{\partial(\Delta b/b_o)}{\partial \eta} = 0 \tag{4.19}$$

together with Eq. (4.16) determines the problem of a thoroughly mixed, or in the terminology of Stommel and Farmer, an "overmixed" estuary. Notice that the conservation equations (4.14), (4.15) yield

$$q_1 \frac{\Delta b}{b_o} = R \tag{4.20}$$

so that a minimum of $\Delta b/b_o$ corresponds to a maximum of the discharge q_1.

The variation of n^2 with η depends on the particular geometry of the estuary, and although this variation may have some quantitative importance we will consider instead the idealized channel with vertical sides so that $n^2 = 1$. Eq. (4.19) then yields

$$\left(1 - \frac{\Delta b}{b_o}\right) = \frac{\eta^2}{(1-\eta)^2} \tag{4.21}$$

In terms of the densimetric Froude numbers we may write

$$F_o^2 = \eta, \quad F_1^2 = 1 - \eta, \quad Q_r^2 = \frac{(1-2\eta)^3}{(1-\eta)^2} \tag{4.22}$$

One special case involves the condition in which the densities of the two fluids are nearly equal. Then from (4.21), $\eta \cong \frac{1}{2}$, $R \cong 0$. Experiments by Stommel and Farmer (1953) and Assaf, Anati and Siegenthaler (1977) confirm the prediction that the two fluids have equal thicknesses in thoroughly mixed estuaries with small fresh water influx and I have derived this result theoretically (Long, 1976). A second special case is one in which $\eta = 0$ so that no salt water enters and fresh water fills the estuary. In this case the solution yields $\Delta b/b_o = 1$, $F_o^2 = 0$ as also required by physical considerations. In the general case (4.22) shows that $\eta \leq \frac{1}{2}$ so that the interface is always at or below mid-depth.

Of interest, particularly in later discussions, is the height ΔH_o of the water surface in the estuary above the level of the ocean surface. If we evaluate the constants in Eqs. (4.6) and (4.7) in the estuary and in the ocean respectively, we get

$$\frac{u_1^2}{2} + g\Delta H = g\Delta H_o \tag{4.23}$$

$$\frac{u_o^2}{2} + g\Delta H - \Delta b h_1 = 0 \tag{4.24}$$

where we now assume that the widths in the ocean and estuary are very large compared to the width of the channel. The constant in Eq. (4.10) is $-g\Delta H_o/\Delta b$ and this equation may then be written

$$\frac{F_o^2 \eta}{2} - \frac{F_1^2(1-\eta)}{2} - (1-\eta) + \beta = 0 \tag{4.25}$$

where

$$\beta = \frac{\Delta H_o}{\bar{h}\Delta\rho/\rho_f} \tag{4.26}$$

Using (4.22) we get

$$\beta = \tfrac{3}{2}\left(1 - \tfrac{4}{3}\eta\right) \tag{4.27}$$

In the overmixed state β ranges between $\frac{1}{2}$ and $\frac{3}{2}$.

We may contrast this strongly mixed case with the case considered in Section 3 in which the mixing is zero. Then $F_o^2 = 0$, $F_1^2 = 1$ and Eq. (4.25) yields $\beta = \frac{3}{2}(1-\eta)$. For future reference we list the two behaviors:

$$F_o^2 = 0, \quad F_1^2 = 1, \quad \beta = \tfrac{3}{2}(1-\eta), \quad Q_f^2 = (1-\eta)^3 \tag{4.28}$$

$$\frac{q_1}{R} = 1, \quad \frac{\Delta b}{b_o} = 1, \text{ weak mixing}$$

$$F_o^2 = \eta\,,\ F_1^2 = (1-\eta)\,,\ \beta = \tfrac{3}{2}(1-\tfrac{4}{3}\eta)\,,\ Q_f^2 = \frac{(1-2\eta)^3}{(1-\eta)^2} \tag{4.29}$$

$$\frac{q_1}{R} = \frac{(1-\eta)^2}{(1-2\eta)}\,,\ \frac{\Delta b}{b_o} = \frac{(1-2\eta)}{(1-\eta)^2}\ \text{, strong mixing}$$

5. Turbulence and Mixing Processes in Stratified Fluids.

We have decided that turbulent mixing of waters of different density (salinity) is a fundamental process in the dynamics of estuaries and we now consider some aspects of turbulence in stably stratified fluids.

Turbulence in a fluid needs an energy source or it will die out. This is especially true in a stably stratified fluid. Thus, letting primes denote departures from mean conditions and using the equations of motion, we may form the energy equation for the turbulent kinetic energy

$$\bar{T}' = \frac{\overline{u'^2}+\overline{v'^2}+\overline{w'^2}}{2} \tag{5.1}$$

If conditions are statistically steady and horizontally homogeneous, we get

$$\frac{\partial}{\partial t}(\bar{T}') = -\frac{\partial}{\partial z}[\,\overline{w'(T'+p'/\rho_f)}\,] - \overline{w'u'}\bar{u}_z - \overline{w'b'} - \epsilon \tag{5.2}$$

where ϵ is the dissipation function, p is pressure and subscript "z" denotes the vertical derivative. When the fluid is stably stratified, i.e., if the mean density (or buoyancy) decreases with height, the turbulence will be accompanied by a buoyancy flux $q = -\overline{w'b'} < 0$ so that this, and the viscous dissipation ϵ, act as sinks of kinetic energy. Energy must come from the first and/or the second term on the rhs of Eq. (5.2). The first is the energy-flux-divergence term and is a basic source term in certain laboratory experiments to be discussed in this section.

The second is always a source term and arises from a conversion of energy of the mean shear of the current to turbulent energy. It is believed to be of fundamental importance in geophysical phenomena.

In a stably stratified estuary in which salinity increases with depth, q will tend to be negative because rising parcels tend to be more salty and heavy and falling parcels tend to be less salty and lighter. One must be careful, however, because of the possibility of wave motions contributing to w' and b'. Thus, if the fluid is stably stratified, it is capable of internal gravity-wave motion in which the basically level density surfaces move up and down in waves. Obviously if the waves do not break, there will be no rupture of these surfaces and therefore, neglecting the very small molecular conduction, no flux of buoyancy (or salt) despite sizable values of w' and b'. The correlation coefficient will be zero. If the waves break, there will be intermittent turbulence superimposed on the wave motion and q will be negative although the correlation coefficient may be much less than one. Negative q means that the kinetic energy tends to decrease because it requires work to lift heavy parcels up and bring light parcels down. There is a tendency in doing this to increase potential energy at the expense of kinetic energy.

To demonstrate this, it is useful to define <u>available potential energy</u> per unit mass (Long, 1970) by considering it to be the kinetic energy per unit mass attained by a parcel of buoyancy $b = b' + \bar{b}(z)$ as it falls from the height z to the height z_o at which its buoyancy b is equal to the mean buoyancy $\bar{b}(z_o)$ at that level. We have $b' = \bar{b}(z_o) - \bar{b}(z) = -\bar{b}_z \xi$ approximately, where $\xi = z - z_o$ and we have assumed that ξ is small compared with the length scale of the vertical

variation of mean buoyancy[1]. Then neglecting disturbance pressure, we may write

$$\frac{dw}{dt} = \frac{d^2\xi}{dt^2} = -b' = \bar{b}_z \xi \tag{5.3}$$

because z_o is a Lagrangian quantity, so that $dz_o/dt = 0$. Integrating, we get

$$w^2/2 - \bar{b}_z \xi^2/2 = \text{const} \tag{5.4}$$

Thus available potential energy may be defined as

$$V' = -\bar{b}_z \xi^2/2 \quad \text{or} \quad V' = b'\xi/2 \tag{5.5}$$

We may also identify q with potential energy changes. The potential energy of a particle of volume V_o and density ρ is $\rho g V_o z$. Let us now define <u>incremental potential energy</u> as $\rho g V_o z - \rho_f g V_o z$ so that this potential energy is zero when the particle has the density ρ_f. If we let V represent the incremental potential energy per unit mass, then to within the Boussinesq approximation, $V = bz$. Since b is nearly conservative, putting $b = b' + \bar{b}$ and assuming no mean vertical velocity, we have

$$\overline{dV/dt} = \overline{w'b'} = -q \tag{5.6}$$

is the average rate of increase of incremental potential energy per unit mass. We may identify this with available potential energy by differentiating the second equation in (5.5) and again assuming $db/dt = 0$. We get

$$dV'/dt = \tfrac{1}{2}b'd\xi/dt - \tfrac{1}{2}\xi d\bar{b}/dt = \tfrac{1}{2}w'b' - \tfrac{1}{2}\xi \bar{b}_z w' = w'b' \tag{5.7}$$

so that

$$\overline{dV'dt} = \overline{w'b'} = -q \tag{5.8}$$

---

[1] This may not always, or even usually, be the case but our development here is only suggestive of the definition in Eq. (5.5).

Comparing (5. 6) and (5. 8), we see that the average rate of increase of incremental potential energy and the average rate of increase of available potential energy are the same.

In application, we can conceive of an energy-containing eddy in the form of a whirl with horizontal axis of rotation, with velocity σ_u and diameter ℓ. It will lift parcels from their level of origin a distance $\xi \sim \ell$ so that $V' \sim \sigma_b \ell$, where σ_b is the rms buoyancy fluctuation. If the turbulence is not decaying, the kinetic energy must be of this order or larger so that $\sigma_b \ell / \sigma_w^2 \leq 1$.

A typical phenomenon in a turbulent, stably stratified fluid is the appearance of thin layers across which density changes abruptly. We have seen that these exist in nature, for example the interface between the river water and the salt water in a salt wedge at the mouth of some rivers. The surprising feature, however, is that turbulence actually sharpens the interface, or at least serves to maintain the interface instead of diffusing it as one might expect from the general diffusive nature of turbulence. An important example is an experiment originaliy by Rouse and Dodu (1955) portrayed in Fig. 5.1. The vessel is filled initially with water with a stable linear density profile. The grid is then activated and turbulence is created in the nearby fluid. The result is a growing turbulent upper layer with a nearly constant mean density separated from the quiescent fluid below by a thin interfacial layer of large density gradient. We sometimes idealize this by considering it a density discontinuity. Actually in this experiment the layer has a thickness of 1-2 cm. In general, the thickness is proportional to the depth of the mixed layer with a constant of proportionality of 1/5-1/6. (Moore and Long, 1971, Wolanski, 1972, Long, 1973, Crapper and Linden, 1974, Wolanski and Brush, 1975, Assaf, Anati and Siegenthaler, 1977) The interface moves away from the grid at a speed called the entrainment velocity u_e.

A detailed understanding of the turbulence in this experiment has not yet been achieved but Linden (1973) has performed allied experiments and has suggested that the large eddies in the upper mixed layer deflect the interface downward, storing potential energy. When this is released by upward motion, a portion of the heavier fluid is ejected into the mixed layer and then carried away by the turbulent eddies, or as in Keulegan's experiment (1949) by the mean current, leaving the interface sharp again.

The experiment of Rouse and Dodu is typical of those without shear and the only source of energy is the energy-flux-divergence term of Eq. (5.2). We will see that similar experiments have been constructed with shear and in these the shear term of Eq. (5.2) is an important energy source.

Cromwell (1960) studied an experiment similar to that of Rouse and Dodu to simulate the pycnocline, but the first reliable data were obtained by Turner (1968) in an experiment in which the lower fluid was agitated and fluid was withdrawn from the stirred layer at a rate adjusted to keep the interface at the same distance from the grid. The entrainment velocity is then defined by $Au_e = Q$ where Q is the volume withdrawn per unit time and A is the cross-sectional area of the tank.

There have been a number of recent experiments similar to those of Rouse and Dodu and of Turner, for example by Brush (1970). Equipment identical to that of Turner was constructed by Wolanski (1972) (see also Wo'·nski and Brush, 1975), and the one-and two-grid experiments were run with stratification caused by heat, salt, sugar, suspensions of sediments and minute silica spheres. Additional experiments have been run in Turner's apparatus by Linden

(1973), Crapper (1973) and Crapper and Linden (1974) using heat and salt. Baines (1975) has studied a similar experiment with entrainment caused by a jet impinging on an interface.

An important finding in the experiments by Turner (1968) may be expressed as

$$u_e/\omega = C[\omega^2/(\Delta b)]^n \qquad (5.9)$$

where ω is the frequency of the oscillating grid and C is independent of ω and Δb. A number of lengths are kept constant in the experiment so that the dimensional quantity C may vary with these. Turner found that for larger values of $\Delta b/\omega^2$, the exponent n = 1 when stratification is caused by temperature differences and n = 3/2 when caused by differences in salt content. Later investigations (Wolanski, 1972) have confirmed these results and, very recently, Crapper and Linden (1974) have shown rather convincingly that the difference in the values of n is due to the influence of the relatively large molecular conductivity k_h in the heating experiments (the coefficient k_s is much smaller for salt). It appears that whenever the n = 1 law describes the entrainment, the thin layer of strong density variation has an inner layer or core in which molecular diffusion is important. Indeed, earlier unpublished experiments by Claes Rooth (Turner, 1973) support this interpretation. Rooth found a 3/2 dependence in heating experiments when larger turbulent velocities are generated. Thus it appears well established that the 3/2 dependence is appropriate for larger Péclet numbers, $Pé = \sigma_u \ell/k_h$ or $\sigma_u \ell/k_s$ where σ_u and ℓ are the velocity and length units of the turbulence. Crapper and Linden suggest a threshhold value of $Pé \cong 200$ when $\sigma_u = \sigma_u'$ and $\ell = \ell'$ are characteristic of the turbulence near the interface. The dependence on Reynolds number, Re, has not been established because of the rather small ranges of Re in the experiments, but both

Wolanski (1972), who varied Re by a factor of three, and Crapper and Linden (1974) report very weak dependence, if any[1]. We may, therefore, write for large Pé and Re, and strong stability,

$$u_e/\omega = C_1\omega^3/(\Delta b)^{\frac{3}{2}}$$

where C_1 is a function of a, D, and the lengths a_1, a_2..., characteristic of the grid. It is convenient to introduce a dimensionless quantity K_n by the definition

$$C_1 = a^4 D^{-\frac{3}{2}} K_n (a/D, a/a_1, a/a_2..) \tag{5.10}$$

and, therefore,

$$u_e/u_* = K_n Ri^{*-\frac{3}{2}}, \quad Ri^* = D\Delta b/u_*^2 \tag{5.11}$$

where $u_* = \omega a$. It is likely that K_n is independent of a/D when this ratio is small. Ri^* is called the overall Richardson number.

The Turner or Rouse and Dodu experiment can be run with an initial two-fluid system in which both layers have a nearly uniform but different density. The interface again moves away from the grid and the system is basically unsteady because the density of the upper fluid is increasing and because the interface is moving. The motion of the interface can be eliminated by introducing fluid of the density of the lower layer into the lower layer at a rate $q_0 = Au_e$. The upper surface of the system can be held stationary by removing an equal volume of the upper brackish water. There will still be an unsteadiness, however, because the density of the upper fluid will still increase. This can be eliminated by adding fresh water to the upper layer with a flux R and removing brackish water at the rate q_1. The following

---

[1]The independence of molecular quantities is common in turbulence (Tennekes and Lumley, 1972). In Turner's original paper (1968), he expressed the belief that the n = 1 law was the fundamental one and that in some manner the very low diffusivity of salt caused the n = 3/2 law. He has changed his mind on the basis of the evidence we present here (Turner, 1973).

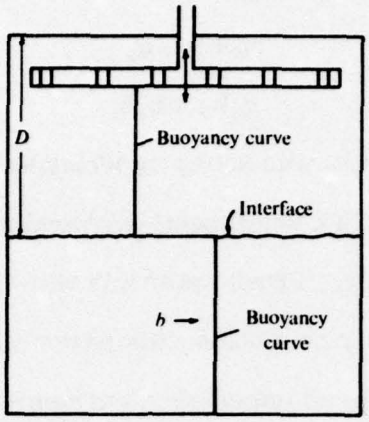

Fig. 5.1 Rouse and Dodu experiment

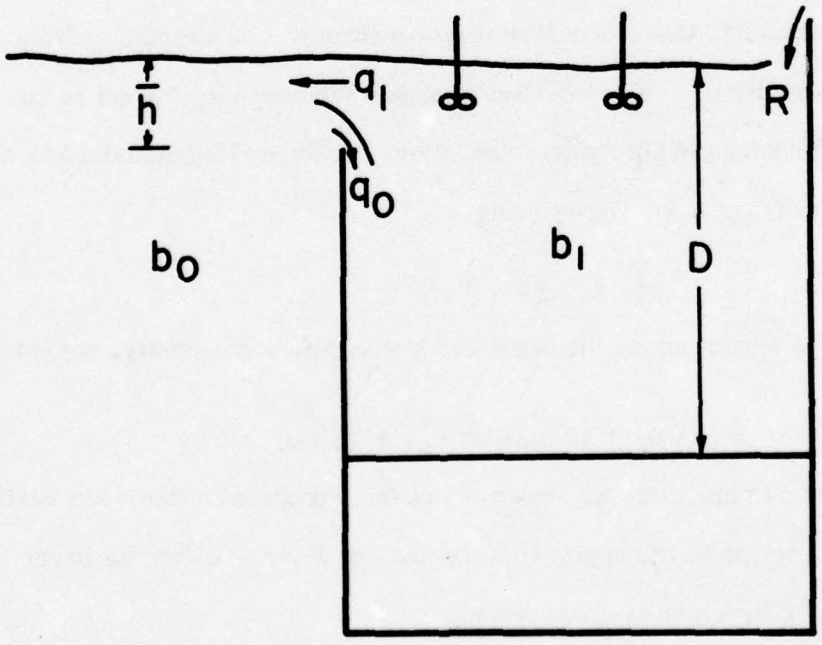

Fig. 5.2 Welander's experiment.

relations must be satisfied to insure a steady-state

$$q_o = Au_e \tag{5.12}$$

$$q_o + R = q_1 \tag{5.13}$$

$$q_o b_o = q_1 b_1 \tag{5.14}$$

An analogous experiment was set up by Welander (1974). It consisted of a large vessel (Fig. 5.2) with a small semi-enclosed portion. The vessel was filled with salt water initially. Fresh water was then introduced into the semi-enclosed region and the upper portions of this region was stirred with a propellor. A steady state developed with an interface in the semi-enclosed region at a depth D and with all conditions in Eqs. (5.12)-(5.14) automatically satisfied. The system resembles an estuary-ocean system; indeed, this was the basic objective of the experiment. Welander only measured the depth D as a function of R and we will discuss these observations in Section 6.

When the interface is stationary, as in an estuary or in Turner's or Welander's experiment, there is a flow of mass through the interface with a mean vertical velocity u_e. We may then consider the buoyancy budget in an element of the thickness of the interfacial layer, arbitrary length and width of the estuary or vessel (Fig. 5.3). Integrating

$$\frac{\partial b}{\partial t} + \nabla \cdot \underset{\sim}{v} b = 0$$

over the element, assuming steady state and horizontal homogeneity, we get

$$-(\bar{w}\bar{b})_o + (\bar{w}\bar{b})_1 - \overline{(w'b')_o} + \overline{(w'b')_1} = 0$$

Since the element is very thin, we may neglect the variation of the mean vertical velocity from the lower to the upper surface and set $\bar{w} = u_e$. Also the lower layer is non-turbulent so that $\overline{(w'b')_o} = 0$. We get

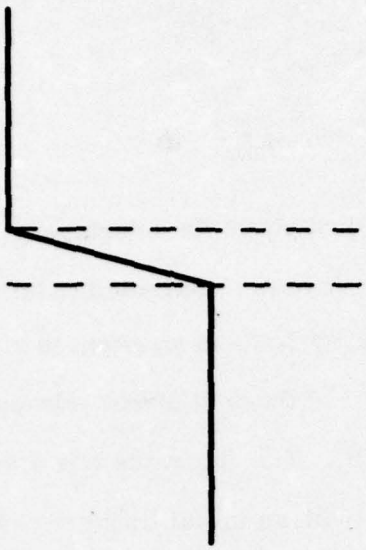

Fig. 5.3 Element of the interface.

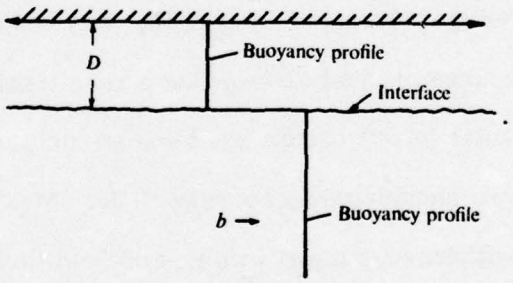

Fig. 5.4 Kato and Phillips experiment.

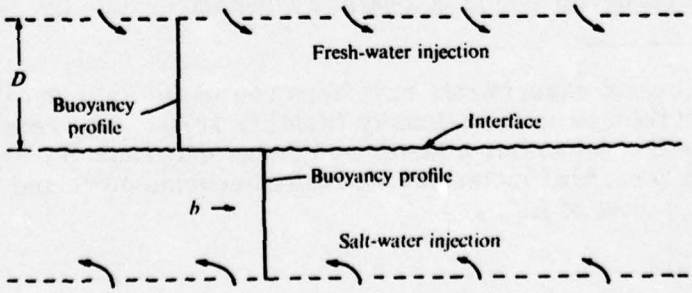

Fig. 5.5 Moore and Long experiment.

$$q = -u_e \Delta b \tag{5.15}$$

where q is the buoyancy flux just above the interface.

Several experiments have been constructed to introduce shearing currents in turbulent density-stratified systems in an effort to simulate atmospheric and oceanic phenomena. The first of these of direct relevance to our discussion was that of Kato and Phillips (1969). The apparatus was a large circular annular channel filled with salt water with an initial linear density gradient. A constant stress $\tau = u_*^2$ was applied by rotating a flat screen at the surface (Fig. 5.4). For larger values of Ri^*, they found

$$u_e / u_* = K_s Ri^{*-1} \tag{5.16}$$

where Ri^* is of the same form as in Eq. (5.11) and Δb is the buoyancy jump from the upper mixed layer to the quiescent region below[1].

An experiment by Moore and Long (1971) was constructed to permit a steady state. In a large channel shaped like a race track, fluid was injected from nearly horizontal jets at bottom (salt water) and top (fresh water) in opposite directions to obtain a shearing current (Fig. 5.5). Mean zero vertical velocities were achieved by withdrawing equal volumes of fluid through numerous holes at bottom and top. At larger values of the density difference, two homogeneous layers existed at top and bottom with an interface in the middle. The salt water in the jets comes from a reservoir and the withdrawn fluid at the bottom is pumped back into the reservoir which is kept at a constant level. The jets at the top are

---

[1] More recent experiments have been run in the Kato and Phillips apparatus using a lower fluid of uniform density (Kantha, 1975). The results do not yield a simple power law but rather a faster and faster decrease of u_e with Ri^*. It is possible, however, that molecular viscosity becomes more and more important at the higher values of Ri^*.

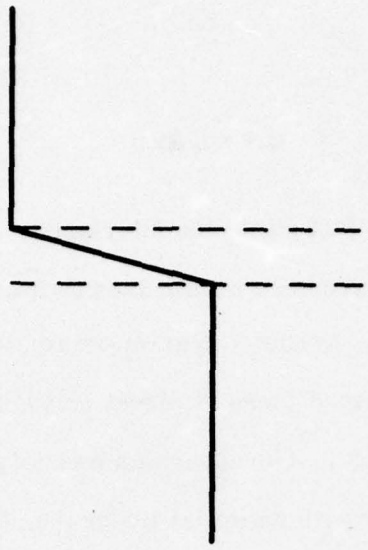

Fig. 5.3 Element of the interface.

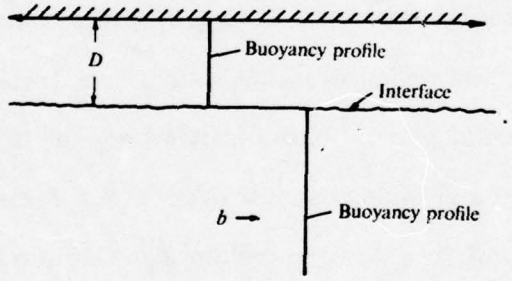

Fig. 5.4 Kato and Phillips experiment.

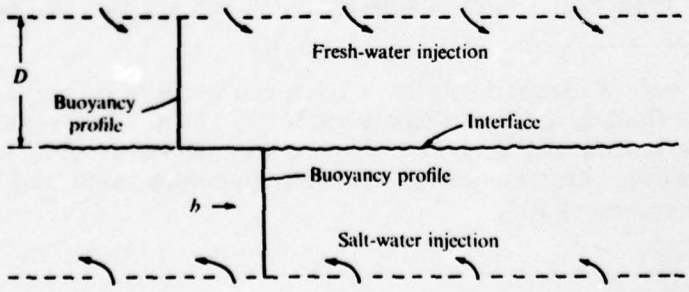

Fig. 5.5 Moore and Long experiment.

of tap water and the slightly salty withdrawn fluid at the top is pumped to waste. Since the fluid returned from the bottom to the reservoir is somewhat less salty than that in the lower jets, salt must be added continually to keep the reservoir at a fixed density. The added salt is transported vertically by the turbulence. The salt flux is known, of course, and this can be used directly to compute the buoyancy flux. The experiment yielded

$$q = -K_3 (\Delta u)^3 / D \tag{5.17}$$

over a range of $D\Delta b/(\Delta u)^2$ of 1 - 60, where Δu is the velocity difference between mean velocities measured near the top and bottom and K_3 is a positive constant of proportionality. If we define the entrainment velocity by $-u_e \Delta b = q$, Eq. (5.17) yields the same result as in Kato and Phillips (Eq. 5.16) if, as seems very likely from a discussion of the Kato and Phillips experiment by Long (1975a), $\Delta u/u_*$ is independent of the Richardson number, where u_*^2 is the constant momentum flux in the tank.

Finally, in a recent experiment by Wu (1973), the source of energy and shear was a current of air blowing over a vessel containing a two-fluid system (Fig. 5.6). Wu also obtained Eq. (5.16) although his coefficient of proportionality was much smaller. He conjectured that this was because of the very different shear produced in a closed container, but Bo Pedersen (private communication) has suggested that the flow at the interface may have been laminar over much of the length.

The different dependence on Ri^* for the two experiments has been the source of perplexity (Turner, 1973, Linden, 1973) because the mixing processes appear to be very similar. Indeed, Linden has stated that the Kato and Phillips data are

also consistent with a -3/2 behavior, although support for the statement seems lacking. We attempt below to construct a unified understanding of the two results.

Turner (1973) has made the valuable suggestion that the erosion of the interface should depend on the properties of the turbulence near the interface, in particular on the rms velocity σ_u' and the integral length scale ℓ' near the interface. Thus, he proposed the form

$$u_e/\sigma_u' = F(Ri_1), \quad Ri_1 = \ell' \Delta b/\sigma_u'^2 \tag{5.18}$$

where possible dependence on other quantities is suppressed and it is assumed that Pé and Re are large. In an attempt to determine the dependence on Ri_1 in his density-interface experiments, in which σ_u' and ℓ' were not measured, Turner used experimental data by Thompson and Turner (1975) in Turner's apparatus with a homogeneous fluid and one grid. They measured σ_u and ℓ at many levels and found that σ_u' was proportional to ω and that ℓ increased linearly with distance from the grid but was independent of ω. Although Thompson and Turner's experiment had no density variation, Turner (1973), Thorpe (1973) and Crapper and Linden (1974) have assumed that the results are directly applicable to the mixing experiments. Thus, at $z = D$ they use

$$\sigma_u'/\omega a = C_2(a/D,\ a/a_1, a/a_2 \ldots) \tag{5.19}$$

$$\ell'/D = C_3(a/a_1, a/a_2 \ldots) \tag{5.20}$$

so that Eq. (5.11) may be written

$$u_e/\sigma_u' = K_4 Ri_1^{-\frac{3}{2}}, \quad K_4 = K_4(a/D, a/a_1, a/a_2 \ldots) \tag{5.21}$$

Neglecting viscosity, the proportionality of σ_u' and ω follows from dimensional analysis but only when the fluid is homogeneous because the presence of an interface introduces a new quantity involving time, namely Δb.

We may also obtain a dependence on Ri_1 for the shearing experiments. With shear and horizontal homogeneity the averaged x-equation of motion yields

$$\partial\tau/\partial z = \partial\bar{u}/\partial t \tag{5.22}$$

where $\bar{u}$ is the mean horizontal velocity at depth z. In the steady-state experiments of Moore and Long (1971), $\partial\tau/\partial z = 0$ and therefore τ is constant with height. Since $\tau = -\overline{u'w'}$, and since the correlation coefficient is very likely to be of order one in the mixed layers, it follows that $u_* = \tau^{\frac{1}{2}}$ is proportional to σ_u'. The interface introduces the length D and it seems reasonable that the eddies fill the whole depth since the density gradient in the mixed layer is weak[1]. Thus we use $\ell' \sim D$ and obtain from Eq. (5.16)

$$u_e/\sigma_u' = K_5 Ri_1^{-1} \tag{5.23}$$

for the Moore and Long experiment. In the experiment of Kato and Phillips, we may use Eq. (5.22) to obtain the increment of τ over the depth D. It is

$$\Delta\tau/\tau \sim UD/T_1 u_*^2 \tag{5.24}$$

where U is the speed of the screen and where T_1 is the time period for a change of depth of order D so that $T_1 \sim D/u_e$. Therefore, ignoring sidewall effects,

$$\Delta\tau/\tau = (U/u_*)(u_e/u_*) \sim Ri^{*-1} \tag{5.25}$$

since, as shown by Long (1975a) U/u_* is independent of Ri^*. This reveals that the stress varies very little over the depth, that $u_* \sim \sigma_u'$, and that Eq. (5.23) again holds.

---

[1] If a fluid is homogeneous, the large, energy-containing eddies tend to be as large as the dimensions of the region (Tennekes and Lumley, 1972). Here the available potential energy may be as large as the kinetic energy but this should not change the order of magnitude of the eddy size. Indeed visual observations indicated that the eddies filled the whole mixed layer in the Moore and Long experiment.

Thus, two different entrainment velocities, Eqs. (5.21) and (5.23), are indicated in the two cases even when the characteristics of the eroding eddies are the same and this is more perplexing than the difference in the exponent of Ri^*. However, a different dependence of σ_u'/u_* or $\sigma_u'/\omega a$ on Ri^* in experiments without shear may be obtained by a plausible argument which casts doubt on the applicability of Thompson and Turner's experiment, in particular Eq. (5.19), to an experiment with a density interface. When there is shear, we have seen that experiment indicates

$$q \sim \sigma_u'^3/D \sim u_*^3/D \tag{5.26}$$

Let us now evaluate q in the mixed layer near the interface. We get $q \sim \sigma_u'\sigma_b'$ where σ_b is the rms buoyancy fluctuation near the interface, and we make the plausible assumption that the correlation coefficient is of order one. Thus

$$\sigma_u'^2/\sigma_b'D \sim 1 \tag{5.27}$$

Assuming again that the eddies fill the whole layer, kinetic energy and available potential energy, $\sigma_b'D$, are of the same order in the mixed layer. Although the layer has very little density variation, this result may be obtained by considering first an experiment with very strong turbulence imposed externally. Then $\sigma_u'^2/\sigma_b'\ell'$ will be very large. As we decrease the turbulence in successive experiments, this ratio will decrease. If turbulence continues to exist, the ratio has a lower limit because $\sigma_u'^2/\sigma_b'\ell' < 1$ would imply that $T' < V'$ and a consequent cessation of the turbulence. It seems unlikely that the ratio will get large again as stability increases so that $\sigma_u'^2/\sigma_b'\ell$ should approach a constant. The argument is equally valid with or without shear. Using Eq. (5.27) when shear is absent

to eliminate σ_b' in the relationship $q \sim u_* \Delta b \sim \sigma_u' \sigma_b'$, the -3/2 law leads to

$$u_*/u_* \sim \sigma_u'^3/Du_* \Delta b \sim u_*^3/(D\Delta b)^{\frac{3}{2}} \tag{5.28}$$

or

$$\sigma_u'/u_* \sim Ri^{*-\frac{1}{6}}, \quad u_* = \omega a \tag{5.29}$$

instead of Eq. (5.19). The decrease of rms velocity with increase of Richardson number when density variations are present may be caused by the weak density gradient in the mixed layer. In a layer as a whole, the slight density variation still has dynamic importance as indicated by the proportionality of kinetic energy and available potential energy and by the fact that q, varying linearly in the layer, has a relatively large value near the interface. Such arguments have been advanced earlier by the author (Long, 1972, 1973).

The energy argument may be amplified. Rouse and Dodu (1955) and others (Kato and Phillips, 1969, Turner, 1973, Wu, 1973) have suggested that the Ri^{*-1} law implies that the change of potential energy is proportional to the energy supply by the external source. Thus, as we have seen, the average rate of increase of potential energy per unit mass is q, so that the rate of increase of potential energy for the system is proportional to qD. In the Kato and Phillips experiment, for example, the rate of working of the external force is τU. If these are proportional,

$$q \sim \tau U/D \sim u_*^3/D \tag{5.30}$$

as in Eq. (5.26). The same conclusion cannot be reached for cases without shear and on this basis it may be argued that the $Ri^{*-\frac{3}{2}}$ law does not conform to any simple energy argument. We may show, however, that the last conclusion is not correctly drawn. In the shearing experiments, the velocity difference is

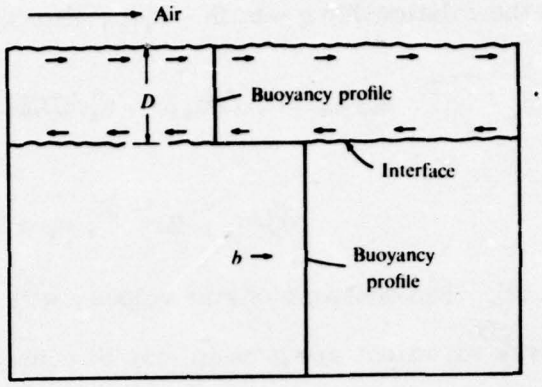

Fig. 5.6 Wu's experiment.

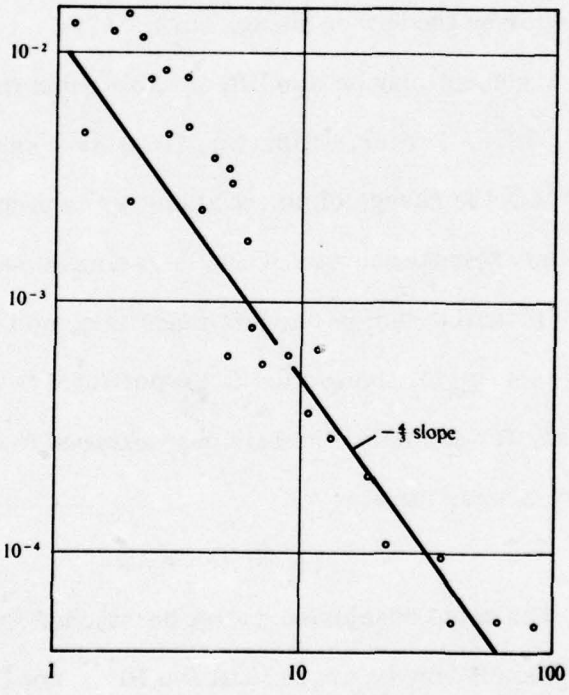

Fig. 5.7 Observations in Wolanski's experiment. The straight line is a plot of the equation $\overline{\Delta b'\Delta b} = \text{const.}\ Ri^{*\,-\frac{4}{3}}$

proportional to $u_* = -(\overline{w'u'})^{\frac{1}{2}}$ (Long, 1975a) and the two energy-source terms in Eq. (5.2) as well as the dissipation ϵ, are of order $\sigma_u'^3/D$ or $\sigma_u'^3/\ell'$ near the interface. If $q \sim u_* \Delta b$ is also of this order, we obtain $u_*/\sigma_u' \sim Ri_1^{-1}$ as in Eq. (5.23). When shear is absent, the single source term is the first term on the rhs of Eq. (5.2) and is also of order $\sigma_u'^3/\ell'$. The Ri_1^{-1} law again implies equality of all sink and source terms. The correct interpretation of experimental results thus seems to be that the turbulence has a character that causes potential energy to increase at a rate proportional to the rate at which kinetic energy is supplied to the region of the interface and not necessarily proportional to the rate of generation of kinetic energy at the external source.

An additional piece of information may be added in relation to experiments without shear. If we assume that the small buoyancy difference $\overline{\Delta b}$ across the mixed layer is of order of the rms buoyancy fluctuation (implying an eddy length scale of the order of the depth of the layer), Eq. (5.27) and Eq. (5.29) lead to

$$\overline{\Delta b}/\Delta b \sim Ri^{*-\frac{4}{3}} \tag{5.31}$$

This quantity was measured by Wolanski (1972) and Wolanski and Brush (1975) for the salt experiments (Fig. 5.7). There is good agreement with Eq. (5.31) especially at higher values of Ri^*.

When there is shear, σ_u' in Eq. (5.27) is of order u_* and σ_b' is of order $\overline{\Delta b}$ so that $\overline{\Delta b}D/u_*^2 \sim 1$ and $\overline{\Delta b}/\Delta b$ is proportional to Ri^{*-1}. Notice also that in the mixed layer the velocity shear is $\bar{u}_z \sim u_*/D$, as shown by Long (1975a). Thus the gradient Richardson number $Ri = \bar{b}_z/(\bar{u}_z)^2$ is of order one in the mixed layer. Observations in the lower mixed layer in the atmosphere (Businger et al. 1971)

indicate that this has a maximum of $Ri_c \tilde{=} 0.20$ and we may speculate that this is the magnitude of Ri in the mixed layer in the experiment. As we have already suggested, $Ri \sim 1$ means that the slight density gradient in the mixed layer has dynamical significance.

We have suggested that

$$u_e/\sigma_u = K_n \sigma_u^2/D\Delta b \qquad (5.32)$$

is a universal law for entrainment with or without shear, where σ_u is the rms velocity at or near the interface. Let us apply this to an experiment without shear, as in Turner's experiment except that the lower quiescent fluid has a linear density gradient. If we also adopt the findings of Bouvard and Dumas (1967) and Thompson and Turner (1975) that σ_u is proportional to $D^{-\frac{3}{2}}$, then since $\Delta b = N^2 D/2$, where N^2 is the buoyancy gradient in the lower fluid, we find that $D \propto t^{2/15}$. This behavior was proposed by Linden (1975) and his experiments with this type of fluid system provided close verification of this time dependence. These experiments, therefore, provide considerable support for the form proposed in Eq. (5.32).

6. Mass and Salt Transfers and Halocline Depths in an Estuary.

With the background of Section 5, we will now consider the effects of finite mixing on the various features of estuarine circulations and distributions. We have in mind a body of water like the Baltic Sea, although the model has variable parameters which permit application to almost any estuary whose mouth has a width small compared to the general horizontal dimensions of the estuary. A comparison is also possible with laboratory experiments designed to produce estuarine circulations.

We will not discuss at any length the practical importance of studies of estuarine circulations and mass distributions. The problem of pollution of waters near the surface obviously demands attention, but another problem of strong interest for the Baltic and many fjord-type estuaries of Scandinavia is the stagnation of the deep water (Fonselius, 1962, 1967, 1969; Gade, 1970). This is associated with the blocking effects of the sill and other obstructions to deep water motion in conjunction with the stabilizing effects of the typical density increase with depth in an estuary associated with temperature and salinity variations in the vertical. The water motions are very slow and therefore even exceedingly weak density increases with depth greatly inhibit vertical motions. The water stagnation implies very weak or zero turbulence in the deep waters and little turbulent mixing with the fluid above. This in turn cuts off the supply of oxygen from the aerated surface water, and the deep layers may ultimately become completely exhausted of oxygen. This has been a progressive development in the deep Baltic over the past 75 years. One station in the central Baltic shows an oxygen saturation decrease from 30% to near 0% during this period at a depth of 160 m (Fonselius, 1969). Fonselius has warned that the Baltic deep water may soon become devoid of life.

The complexities of real estuaries have been emphasized by many authors, e. g. Pritchard (1956), Fonselius (1969), Gade (1970) and Welander (1974). The Baltic, for example, is connected to its source of salt water, the Kattegat, by the Danish Belts and the Öresund. This in itself is a great complication compared to our model which is portrayed in part in Fig. 6.1 . The model has a single connection to the ocean. When we compare the model and the Baltic we consider

only the Store Belt which, in fact, is mainly responsible for the fluxes into and out of the Baltic. We take the minimum width W = 15 km for the Belt and a mean depth at this section $\bar{h}$ = 18 m. In the model, the estuary waters and the flow at the mouth are divided into two layers by a thin halocline. This is not a bad approximation for the Baltic which has a permanent halocline of thickness 10 m at a depth D $\tilde{=}$60 m, although there certainly are vertical and horizontal gradients of salinity above and below the halocline[1]. For example, the salinity of the inflowing water in the Store Belt is about 17.5$^{o}/_{oo}$ compared to 11$^{o}/_{oo}$ in the Baltic sea deep water although the model ignores this and assumes no mixing as the ocean water pours into the basin. The salinity of the upper layer in the Baltic is about 7$^{o}/_{oo}$. The model assumes that the inflowing water is all ocean water; by way of comparison, some of the outflowing Baltic water mixes with the Skagerak water and recirculates back into the Baltic.

The water balance of the Baltic region involves a close equality of precipitation and evaporation so that the fresh water influx R is equal to the river runoff which we take to be R = 1.49 x 10^{10} cm^3/sec. The outflowing water has a flux q_1 which is about twice the magnitude of R (Brogmus, 1952).

Estuarine circulations are usually very small, of order of centimeters per second or less, and this suggests a considerable importance of friction. This has been confirmed by many investigations (e.g. Pritchard, 1956) and is treated in Section 7. At a narrow mouth, however, speeds increase very considerably, inertial, pressure and gravity forces become comparable (Long, 1975b) and

---

[1] Notice that the ratio of the thickness of the halocline to its depth is 1/6 in accordance with laboratory evidence referred to on page 22.

friction becomes relatively much less important. In the present Section we confine attention to flows near the mouth and we neglect friction entirely in this region.

As we discussed in Section 5, we adopt the mixing law, Eq. (5.32)

$$\frac{u_e}{\sigma_u} = K_n \frac{\sigma_u^2}{D\Delta b} \tag{6.1}$$

where we estimate $K_n \cong 0.093$ from experiments (Long, 1975b) and σ_u is the rms horizontal turbulent velocity near the interface. It is instructive to compute the entrainment velocity for two choices of the quantities in Eq. (6.1). In the Baltic, for example, if we use the salinity difference of $4^o/_{oo}$, we get $\Delta b \cong 3.2$ cm/sec^2 The turbulent intensity is very uncertain and u_e is sensitive to its value, but if we use an estimate $\sigma_u = 1.4$ cm/sec suggested by a discussion below, and $D = 60$ m, we get $u_e = 1.1$ cm/day. This suggests very slow adjustments to changes in fresh water supply and turbulent intensities. In estuaries in which tidal effects are large σ_u may be much larger. If we use $\sigma_u = 10$ cm/sec, $D = 15$ m, $\Delta b = 10$ cm/sec^2, more appropriate, say, to estuaries in British Columbia (Pickard & Rodgers, 1959), we obtain $u_e = 5$ m/day and adjustments to changes will be very rapid.

The entrainment velocity in the estuary may be written $u_e = q_o/A$ (Fig. 6.1), or A is the area of the halocline in the estuary. Using Eqs. (4.14) and (4.15), we have

$$q_o = \frac{(1-\Delta b/b_o)R}{\Delta b/b_o} \tag{6.2}$$

Then Eq. (6.1) becomes

$$Q_f\left(1-\frac{\Delta b}{b_o}\right) = \frac{1}{D_* M}, \quad D_* = \frac{D}{\bar{h}} \tag{6.3}$$

where Q_f is given in Eq. (4.17) with $\bar{W}_1$ and $W_o = \bar{W}$ and

$$M = \frac{b_o^{\frac{3}{2}} \bar{h}^{\frac{5}{2}} \bar{W}}{AK_n \sigma_u^3} \tag{6.4}$$

We may now relate this to the discussion in Section 4. The results in Eq. (4.28) apply to the case of zero mixing, i.e., $M = \infty$. The results in Eq. (4.29) imply $\sigma_u \to \infty$ or $M = 0$. Obviously then, $\beta = \Delta H_o / \bar{h}\left(\frac{\Delta\rho}{\rho_f}\right)$, equal to

$$\beta = \tfrac{3}{2}(1-\eta) \ , \ M = \infty \tag{6.5}$$

$$\beta = \tfrac{3}{2}(1-\tfrac{4}{3}\eta), M = 0 \tag{6.6}$$

in the two extreme cases, will be some function of η and M for finite mixing. I don't see any way to find this relationship rigorously but a simple form which satisfies the two extremes is

$$\beta = \tfrac{3}{2}\left[1 - \frac{\eta[4+3M^s f(\eta)]}{3[1+M^s f(\eta)]}\right] \tag{6.7}$$

where s is a constant and $f(\eta)$ is arbitrary. There are additional requirements which must be satisfied. Thus as $\sigma_u \to 0$, $M \to \infty$, it follows from Eq. (3.5) that

$$\frac{D}{\bar{h}} \to \tfrac{3}{2}(1-\eta) \tag{6.8}$$

Eqs. (4.13) and (4.25) lead to

$$F_o^2 = 3 - 3\eta - 2\beta \tag{6.9}$$

so that (6.7) and (6.9) lead to

$$\frac{q_o^2}{\bar{h}^3 \eta^3 \Delta b \bar{W}^2} = \frac{\eta}{1+M^s f(\eta)} \tag{6.10}$$

Using

$$q_o = \frac{AK_n \sigma_u^3}{D\Delta b} \tag{6.11}$$

Eq. (6.10) becomes

$$\frac{A^2 K_n^2 \sigma_u^6}{D^2 \bar{h}^3 \eta^3 (\Delta b)^3 \bar{W}^2} = \eta \left[1 + \left(\frac{b_o^{\frac{3}{2}} \bar{h}^{\frac{5}{2}} \bar{W}}{A K_n \sigma_u^3} \right)^s f(\eta) \right]^{-1} \tag{6.12}$$

As $\sigma_u \to 0$ all other quantities remain finite and we see that $s = 2$, $\Delta b \to b_o$. Using (6.8), we obtain

$$f(\eta) = \frac{9}{4} \eta^4 (1-\eta)^2 \tag{6.13}$$

We get

$$\beta = \tfrac{3}{2} \left[1 - \frac{\eta [16 + 27 M^2 (1-\eta)^2 \eta^4]}{3 [4 + 9 M^2 (1-\eta)^2 \eta^4]} \right] \tag{6.14}$$

A combination of (4.16), (6.2), the definition of F_o^2, (6.9) and (4.17) leads to

$$Q_f^2 = \frac{\left(\frac{\Delta b}{b_o}\right)^3 (1-\eta)^3 [4 + 9 M^2 (1-\eta)^2 \eta^4 - 4\eta]}{[4 + 9 M^2 (1-\eta)^2 \eta^4]} \tag{6.15}$$

$$\left(1 - \frac{\Delta b}{b_o}\right)^2 = \frac{4\eta^4}{(1-\eta)^3 [4 + 9 M^2 (1-\eta)^2 \eta^4 - 4\eta]} \tag{6.16}$$

D_* is given by

$$D_* = \frac{1}{Q_f M \left(1 - \frac{\Delta b}{b_o}\right)} \tag{6.17}$$

Equations (6.14)-(6.17) determine all unknowns, given the fresh water flux ratio Q_f and the mixing number M.

The form of the solution is rather complicated but a simple example of a solution of Eqs. (6.14)-(6.17) is an estuary with an infinitely deep sill, i.e., $\bar{h} \to \infty$. The solution then depends on a single non-dimensional number

$$M' = \frac{R^{\frac{5}{3}} b_o^{\frac{2}{3}}}{A K_n \sigma_u^3 \bar{W}^{\frac{2}{3}}} \tag{6.18}$$

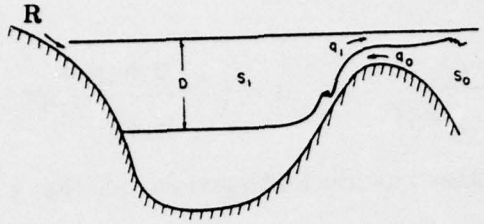

Fig. 6.1 Estuary with a sill and/or contraction

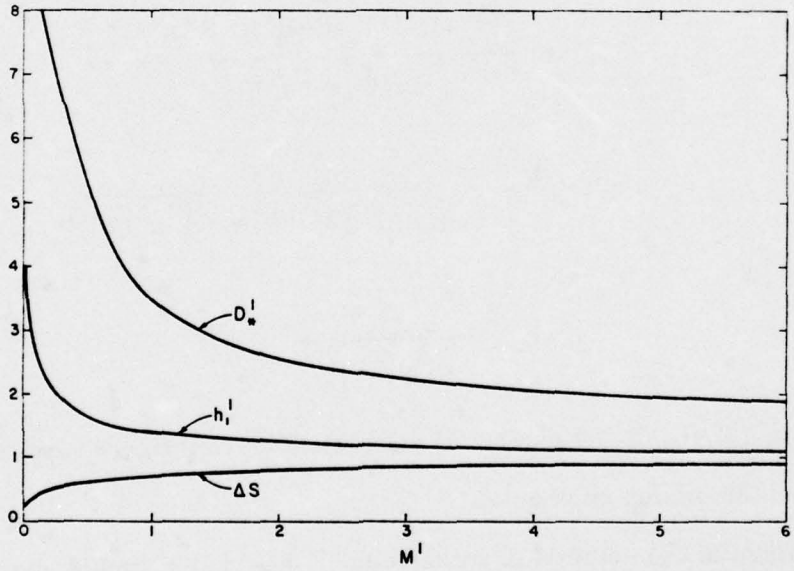

Fig. 6.2 Interface and halocline depths and salinity differences for an infinitely deep estuary. D'_* and h'_1 are defined in Eq. (6.19). ΔS is the same as $\Delta b/b_0$.

Using the definitions

$$D'_* = \frac{D b_o^{\frac{1}{3}} \bar{W}^{\frac{2}{3}}}{R^{\frac{2}{3}}} , \quad h'_1 = \frac{h_1 b_o^{\frac{1}{3}} \bar{W}^{\frac{2}{3}}}{R^{\frac{2}{3}}} \tag{6.19}$$

where h_1 is the depth of upper layer at the constriction. We get

$$D'_* = -\frac{1}{M'(1-\frac{\Delta b}{b_o})} , \quad h'_1 \frac{\Delta b}{b_o} = 1, \quad (1-\frac{\Delta b}{b_o}) = \frac{2}{3M'h'^{\frac{5}{2}}_1} \tag{6.20}$$

Results are shown in Fig. (6.2). The depth of the interface at the mouth h_1 and the halocline depth D increase monotonically as M' decreases (mixing increases). D is about twice as large as h_1 for larger M' over most of the range of M'. The salinity of the outflowing fluid increases monotonically as the mixing increases and the fresh-water flux decreases. The flux of the outflowing fluid changes very slowly with M' over most of the range, $q_1/R = (\Delta b/b_o)^{-1}$ increasing from 1.0 to 1.5 as M' decreases from infinity to $M' \cong 1$. Below $M' = 1$, q_1/R increases more rapidly but only begins to exceed 2.0 when M' drops below $M' = 0.1$.

When the sill depth is finite, Eqs. (6.14)-(6.17) reveal a common behavior for all values of M, namely that the halocline is very deep for both small and large values of the fresh-water flux R, with a minimum at a value of Q_{fm} determined by M. The quantity Q_{fm} decreases with M; for example $Q_{fm} = 0.244$ at small M, $Q_{fm} = 0.08$ at $M = 100$ and $Q_{fm} = 0.03$ at $M = 1,000$. The behavior of D_* as a function of Q_f is shown in Fig. (6.3) and (6.4) for smaller and larger values of M, respectively. When M exceeds 100 or so there is little change in the behavior over most of the range of Q_f except near Q_{fm}. There the halocline depth continues to decrease strongly as M gets still larger.

Fig. (6.5) shows an experiment by Welander (1974) similar to the model of this paper. Data are lacking to permit a careful comparison, but $M = 8$ seems a good choice. Constants were chosen to force agreement near the minimum point.

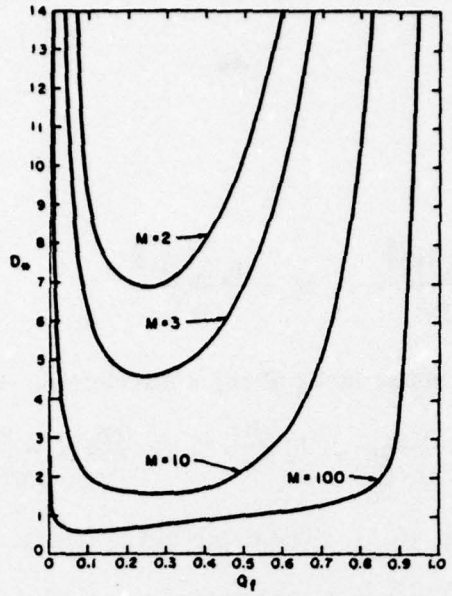

Fig. 6.3 Halocline depth as function of fresh-water influx for smaller values of M.

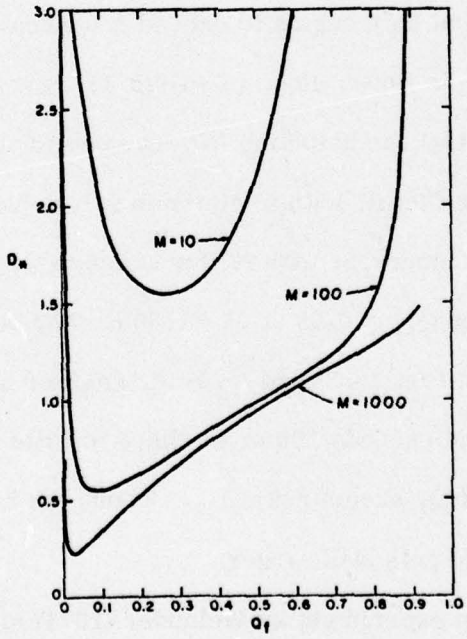

Fig. 6.4 Halocline depths as function of fresh-water influx for larger values of M.

The agreement is quite good except for small values of R where entrainment velocities are very small and the experiments may not have been in a steady state. An additional factor is the decrease of σ_u near the interface as D increases and the interface gets further and further away from the source of energy (stirrers). This effect is not included in the theory and would tend to reduce D. The tendency for a minimum depth of the halocline has been observed by Tully (1949) in Alberni Inlet as we see in Fig. (6.6). The theoretical curve corresponds to M = 0.

The quantity β varies with Q_f and M as seen in Fig. (6.7). It is interesting to note that $\beta\Delta S \propto \Delta H_o/\overline{h}$ varies very little with M. Indeed, one would anticipate that this quantity would vary more sensitively with Q_f.

The influx of ocean water is negligible for M > 100 or so. As mixing increases, Q_o, defined by

$$Q_o = \frac{q_o}{b_o^{\frac{1}{2}} \overline{h}^{\frac{3}{2}} \overline{W}}$$

increases. Q_o rises with increase of Q_f, reaches a naximum and then decreases. Examples are shown in Fig. (6.8). The curves for M < 3 or so do not differ very much from the curve shown for M = 0.10. This typical behavior of Q_o appears in other theories of estuaries, for example Kullenberg (1955).

The salinity of the outflowing fluid increases as the fresh water influx decreases. This was also pointed out by Kullenberg. Fig. (6.9) shows the curves for two values of M. Decreases in mixing intensities accompany decreases in salinity, as expected.

An estimation of M for various applications is important but M is

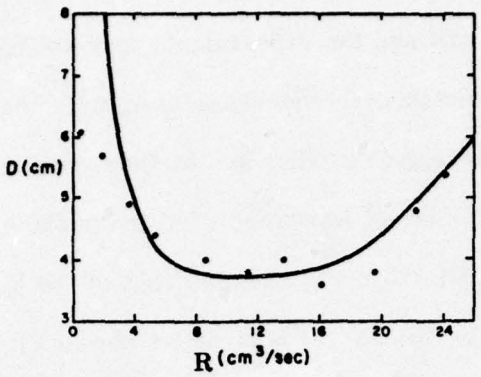

Fig. 6.5 Halocline depths in Welander's experiment.

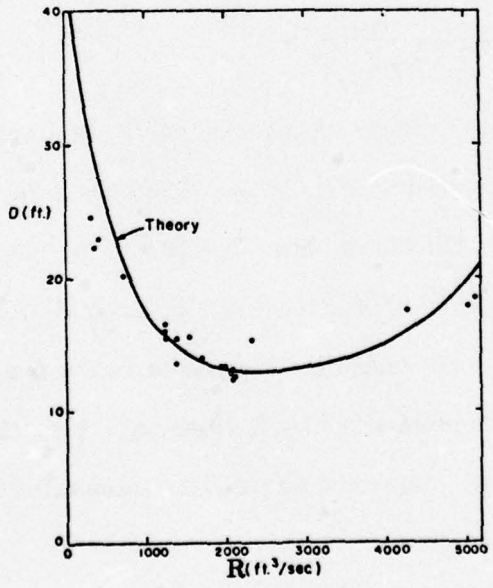

Fig. 6.6 Observations of halocline depths in Alberni Inlet.

extremely sensitive to σ_u and σ_u is difficult to estimate. We may make the following computations for the Baltic Sea: Fonselius (1969) gives the ratio $q_1/R \cong 2$. We may compute Q_f from Eq. (4.10) with the constant equal to $-g\Delta H_o/\Delta b$ using the data of Fonselius of $R = 1.49 \times 10^{10} cm^3/sec$ and width $\bar{W} = 15$ km, depth $\bar{h} = 18$ m for the Store Belt. The appropriate value of b_o corresponds to a salinity in the lower layer of 17.5‰ or $b_o = 14 cm/sec^2$. This leads to $Q_f = 0.0348$. Finally $D/\bar{h}$ for the Baltic is 60/18 or 3.33. If we use the last two figures, we obtain close agreement for a value of M = 12. The computations yield $Q_f = 0.0346$ and $D/\bar{h} = 3.45$. The value of q_1/R, however, is 3.29 which is considerably too large. The value of M = 12 permits us to compute σ_u using $A = 3.1 \times 10^{15} cm^2$. We obtain $\sigma_u = 1.4$ cm/sec which is, perhaps, reasonable.

One may speculate regarding the changes in the Baltic over the past 75 years as described by Fonselius. The stability of the Baltic has apparently increased, because, although the salinity of the upper and lower layers have both increased, the salinity of the lower layer has increased somewhat more. This stability increase may be related to the reduction of oxygen in the deep Baltic. R has decreased about 15% over this period and Fonselius ascribes the increase of salinity in the Baltic as a whole to this decrease of R. A further change has been a decrease in the depth of the halocline from 80 m to 60 m over the period. According to present theory, for the value of M = 12 and the other conditions of the Baltic, a decrease of R with all other factors held constant should have resulted in an increase of D. However, as we have seen, D is most sensitive to σ_u. Since precipitation and runoff have decreased, this implies a

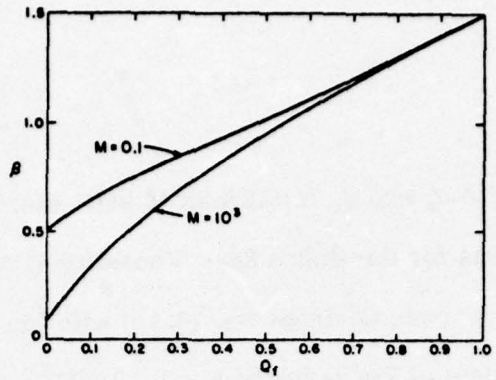

Fig. 6.7 Variations of β with Q_f and M.

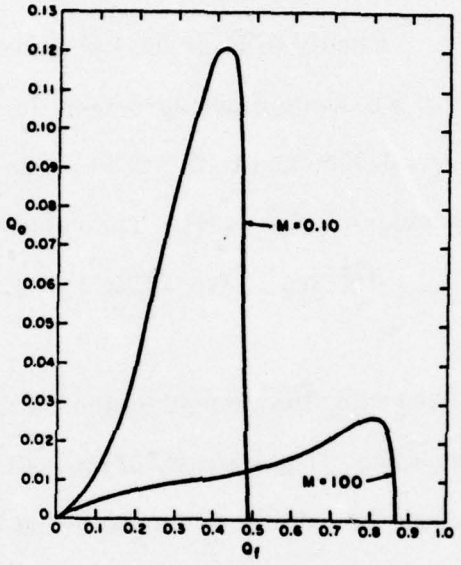

Fig. 6.8 Variations of ocean water flux with fresh water influx.

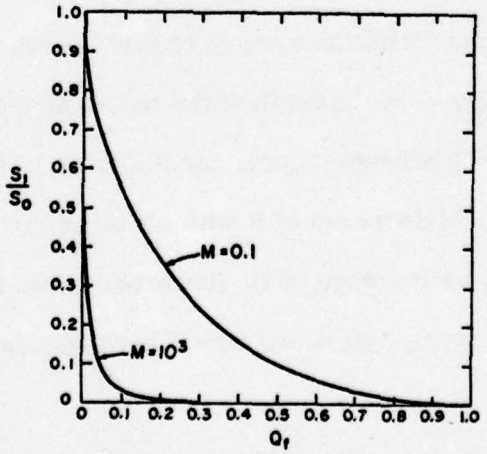

Fig. 6.9 Salinity of brackish water as a function of fresh water influx.

decrease of storminess over the Baltic as asserted, in fact, by Fonselius, and a decrease of σ_u. This could have been overriding and serves to explain the decrease of D. Notice that only long period changes in σ_u are involved because we have decided that the response of the halocline depth to changes is very slow.

7. Circulations and Density Distributions in a Deep, Strongly Stratified, Two-Layer Estuary.

In Section 6 we considered an estuary of a rather general type except that the connection to the open sea has such a character that (1) the flow in this portion of the estuary (mouth) is perfect fluid flow and (2) conditions become critical at one section of the mouth. Our investigation derived an expression for the depth of the halocline in the estuary proper but other than this nothing was found out about the circulations and salt distributions in the estuary except near the mouth. We now investigate (Long, 1975b) conditions throughout an estuary without the two assumptions mentioned above. For simplicity we assume that the estuary is infinitely deep everywhere. As it develops, this means that the halocline depth is small compared to the depth of the estuary. This is not a bad assumption in many cases, for example in fjords in British Columbia and Alaska, but the model does not include the situation in some Scandanavian fjords in which there is a sill whose depth is of the order of the depth of the halocline.

The model (Fig. 7.1) has a well-mixed upper layer and a deep, non-turbulent uniform lower layer of the density of sea water. The width of the estuary is W(x) and the sides are vertical. The free surface is given by $z = H$ and the interface by $z = D_0(x)$. The upper layer has a mean depth D(x). The variation of H along the estuary provides an important component of the pressure gradient force but incre-

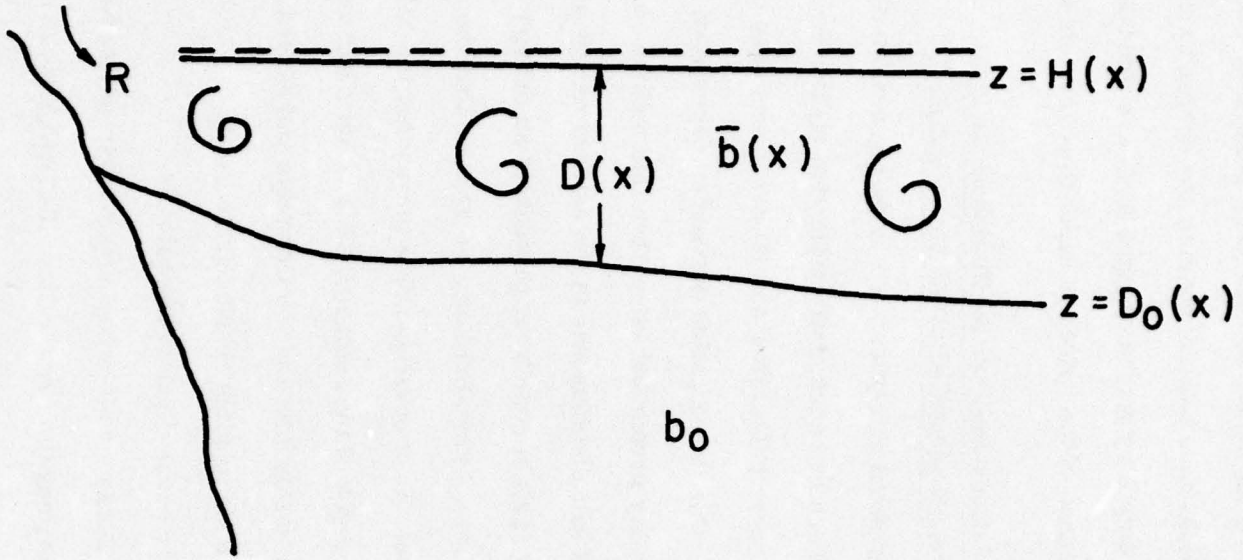

Fig. 7.1 Model of estuary.

ments in H are of the order of 10 centimeters over tens of kilometers and so may be neglected elsewhere in the argument and H taken to be a constant. The vertical variation of the buoyancy is confined to a thin, interfacial zone whose thickness is neglected, but the mean buoyancy varies continuously with x in the upper layer as the water flowing out to sea becomes more and more brackish. In general, a symbol such as b denotes an ensemble average or average over a long time, and $\bar{b}$ denotes an average of b over the vertical cross-section in the upper fluid.

The buoyancy difference between the two layers is Δb and varies along the channel because the buoyancy of the upper layer varies. The rms turbulent velocity in the upper layer is σ_u and we assume that σ_u is uniform in the layer. To be definite we take σ_u to be the rms horizontal velocity component along the x-axis. The non-dimensional quantity $Ri_2 = D\Delta b/\sigma_u^2$ has the form of a Richardson number. If we take as typical values, $D = 10^3$ cm, $\Delta b = 25$ cm sec^{-2}, $\sigma_u = 10$ cm sec^{-1}, we get $Ri_2 = 250$. We have taken a rather high value for σ_u so that Ri_2 will usually be greater than this. It is reasonable then to assume that the estuary is strongly stratified in the sense that $Ri_2 \gg 1$.

Conservation of mass for a region of the upper layer of length Δx, width W, and thickness D yields

$$\Delta(WD\bar{u}) = \iint v_n \, da \qquad (7.1)$$

where $\bar{u}$ is the mean velocity over the cross-section of the upper layer, da is an element of area of the interface, and the integral is over the interfacial boundary of the region. The normal velocity into the layer, v_n, is zero when there is no mixing. We have already assumed, however, that turbulence exists in the upper layer, and we may identify v_n with the entrainment velocity so that with use of Eq. (5.32), Eq. (7.1) becomes

$$\frac{d}{dx}(WD\bar{u}) = \frac{K_n \sigma_u^3 W}{D\Delta b} \tag{7.2}$$

The pressure in the lower layer is

$$\frac{p}{\rho_f} = g(H-z) + \bar{b}(H-D_o) + b_o(D_o-z) \tag{7.3}$$

If we assume, as indicated above, that the lower fluid has a depth large compared to that of the upper fluid, horizontal accelerations will be negligible and the longitudinal pressure gradient is zero in this layer (Gade, 1974). Then

$$gH_x = \Delta b \frac{dD}{dx} - D\frac{d\bar{b}}{dx} \tag{7.4}$$

Let us now integrate the horizontal equation of motion,

$$\frac{\partial u}{\partial t} + \nabla \cdot u\underset{\sim}{v} = -\left[gH_x + (H-z)\frac{d\bar{b}}{dx} \right] - \frac{\partial(\overline{u'u'})}{\partial x} - \frac{\partial}{\partial y}(\overline{u'v'}) - \frac{\partial}{\partial z}(\overline{u'w'}) \tag{7.5}$$

over a region of the upper fluid of length Δx, width W and thickness D. We get

$$\frac{1}{W\Delta x}\iiint \nabla \cdot \underset{\sim}{v} u dV = -D\Delta b \frac{dD}{dx} + D^2 \frac{d\bar{b}}{dx} - \tau_i - \int_{D_o}^{H} \frac{d\bar{b}}{dx}(H-z)dz \tag{7.6}$$

where the pressure in the upper layer is given by $p = \rho_f g(H-z) + \rho_f \bar{b}(H-z)$ and where τ_i is very nearly equal to the average stress at the interface. We assume[1] $\tau_i = K\bar{u}^2$ where K is the drag coefficient. A term involving the horizontal rate of change of τ_x has been omitted in Eq. (7.6) because the turbulence is assumed to

[1] This is a standard assumption for example in flow in pipes. The stress is basically equal to $-\overline{u'w'}$ and in typical shearing flows $\sigma_u/\bar{u}$ and $\sigma_w/\bar{u}$ are small and vary very slowly with Reynolds number and so are taken to be constants. The stress then is proportional to $\bar{u}^2$ with a small coefficient of proportionality. In the present case it is likely that $\sigma_u/\bar{u}$ and $\sigma_w/\bar{u}$ are of order one so that K is of order one. We assume this later.

be uniform in the upper layer. If u_1 is the average horizontal velocity at the bottom of the upper layer, the integral on the ℓhs of Eq. (7.6) may be written

$$\frac{1}{W}\frac{d}{dx}\iint uudzdy - u_e u_1 \tag{7.7}$$

The ratio of $u_e u_1$ to the term τ_1 in Eq. (7.6) is of order $u_e D/K_m$, or less, where K_m is the eddy viscosity in the upper fluid near the interface. We estimate K_m as $\ell\sigma_u$ where ℓ is the eddy size. If we use observations of flow in pipes, we may estimate $\ell \cong D/3$ (Hinze, 1959). Using

$$u_e \cong \frac{1}{10}\frac{\sigma_u^3}{D\Delta b}$$

the ratio is approximately $0.3\ \sigma_u^2/D\Delta b$ which we have assumed to be small. Thus the second term in Eq. (7.7) may be neglected.

Let us now write

$$\iint uudzdy = \gamma\bar{u}\bar{u}DW \tag{7.8}$$

The quantity γ depends on the velocity distribution in the layer. If the velocity is uniform, $\gamma = 1$. Other physically reasonable assumptions yield values greater than 1 but less than 2 or so. Our analysis does not yield a precise value for γ, but we find that γ occurs in combination with other equally uncertain constants of the problem so that it seems pointless to attempt to refine this portion of the argument.

Eq. (7.6) becomes

$$\frac{\gamma}{W}\frac{d}{dx}(\bar{u}\bar{u}WD) = \frac{D^2}{2}\frac{d\bar{b}}{dx} - D\Delta b\frac{dD}{dx} - K\bar{u}^2 \tag{7.9}$$

where we have assumed that γ is constant. We have two additional equations involving the flux of mass and buoyancy across an entire section:

$$\bar{u}\bar{b}\,DW + q_o b_o = 0 \tag{7.10}$$

$$q_o + \bar{u}DW = q_f W_h \tag{7.11}$$

where q_o is the mass flux over the cross-section in the lower layer, $R = q_f W_h$ is the fresh water influx and W_h is the width at the head of the estuary. We have neglected horizontal diffusion of buoyancy[1] in Eq. (7.10).

Let us now non-dimensionalize using the following quantities:

$$Q = \frac{\bar{u}DW}{q_f W_h}\ ,\quad Q_o = \frac{q_o}{q_f W_h}\ ,\quad \xi = \frac{x\sigma_u}{q_f}\ ,\quad \eta = \frac{D\sigma_u}{q_f} \tag{7.12}$$

$$\delta = \frac{b_o - \bar{b}}{b_o}\ ,\quad m = \frac{\gamma\sigma_u^3}{b_o q_f}\ ,\quad \lambda = \frac{W}{W_h} \tag{7.13}$$

Equations (7.2), (7.9), (7.10) and (7.11) become

$$Q_o = 1 - \frac{1}{\delta}\ ,\quad Q = \frac{1}{\delta} \tag{7.14}$$

$$\frac{dQ}{d\xi} = \frac{K_n m\lambda}{\gamma\eta\delta} \tag{7.15}$$

$$\frac{1}{\lambda}\frac{d}{d\xi}\left(\frac{Q^2}{\eta\lambda}\right) = -\frac{1}{2m}\eta^2\frac{d\delta}{d\xi} - \frac{K}{\gamma}\frac{Q^2}{\lambda^2\eta^2} - \frac{1}{m}\eta\delta\frac{d\eta}{d\xi} \tag{7.16}$$

We may also write Eqs. (7.14)-(7.16) as

$$Q = \frac{1}{\delta}\ ,\quad Q_o = 1 - \frac{1}{\delta} \tag{7.17}$$

$$\frac{\eta}{\lambda Q}\frac{dQ}{d\eta} = \frac{K_n m}{\gamma}\frac{d\xi}{d\eta} \tag{7.18}$$

$$\frac{d}{d\eta}\left(\frac{Q^2}{\eta\lambda}\right) = -\frac{K}{mK_n\lambda^2}\frac{Q}{\eta}\frac{dQ}{d\eta} + \frac{\lambda}{2m}\frac{\eta^2}{Q^2}\frac{dQ}{d\eta} - \frac{\lambda}{m}\frac{\eta}{Q} \tag{7.19}$$

---

[1] The neglected quantity is of order $\overline{u'b'}D$. The ratio of this to $\bar{u}\bar{b}D$ is $\overline{u'b'}/\bar{u}\bar{b} \sim \sigma_b/\bar{b}$ since, as we discuss later, $\sigma_u \sim \bar{u}$. If the horizontal eddy dimension is of the order of the width, σ_b is of the order of the longitudinal mean buoyancy variation over a distance W. This is small compared to $\bar{b}$ if the estuary is long compared to the width.

7.2 The Solution for an Estuary of Uniform Width.

Let us consider the solution of (7.19) when $\lambda = 1$, i.e., when the estuary has a uniform width. If we use a new dependent variable $\zeta = \eta^3/Q^3$, and a new independent variable, $\ell n \eta$, we obtain

$$\frac{\frac{2}{3} + \frac{K}{3mK_n} - \frac{\zeta}{6m}}{\left(1 + \frac{K}{mK_n}\right)\zeta + \frac{\zeta^2}{2m}} d\zeta = d\,\ell n\,\eta$$

The integral of this is

$$\frac{\left(\frac{2}{3} + \frac{K}{3mK_n}\right)}{\left(1 + \frac{K}{mK_n}\right)} \ell n \left[\frac{\zeta}{1 + \frac{K}{mK_n} + \frac{\zeta}{2m}}\right] - \frac{1}{3}\,\ell n\left(1 + \frac{K}{mK_n} + \frac{\zeta}{2m}\right) = \ell n\,\eta + \text{const}$$

Using new constants,

$$s = 1 + \frac{1}{1 + \frac{K}{mK_n}} \quad , \quad C^3 = \frac{1/2m}{1 + \frac{K}{mK_n}} \tag{7.20}$$

the solution is

$$\eta = \frac{\zeta^{\frac{s}{3}}}{(1 + C^3\zeta)^{\frac{s+1}{3}}} + \text{const} \tag{7.21}$$

Imposing the boundary condition that $\eta = \eta_h$ at the head of the estuary where $Q = 1$, Eq. (7.21) becomes

$$\frac{\eta}{\eta_h} = \left(\frac{\zeta}{\eta_h^3}\right)^{\frac{s}{3}} \left(\frac{1 + C^3\eta_h^3}{1 + C^3\zeta}\right)^{\frac{s+1}{3}} \tag{7.22}$$

The quantity ξ may be found by integrating Eq. (7.18). We get

$$\xi = \frac{\gamma}{mK_n} \int_{Q_*}^{Q} \frac{\eta}{Q}\, dQ \tag{7.23}$$

where we choose Q_* to be the flux at an arbitrary section at which $\xi = 0$.

We may simplify the problem considerably by the new definitions

$$\zeta' = C^3 \zeta, \quad \eta' = CQ_h' \eta, \quad Q' = Q_h' Q, \quad \xi' = \frac{mK_n}{\gamma} CQ_h' \xi \tag{7.24}$$

where we denote by Q_h' the value of Q' at the head of the estuary. We then obtain

$$\eta' = \frac{\zeta'^{\frac{s}{3}}}{(1+\zeta')^{\frac{s+1}{3}}}, \quad \zeta' = \frac{\eta'^3}{Q'^3} \tag{7.25}$$

$$\xi' = \int_{Q_*'}^{Q'} \frac{\eta'}{Q'} dQ', \quad Q_h' = \frac{C^{s-1} \eta_h^{s-1}}{(1+C^3 \eta_h^3)^{\frac{s+1}{3}}} \tag{7.26}$$

where $Q_*' = Q_h' Q_*$. Notice that $1 < s < 2$ tending to $s = 1$ as σ_u decreases to zero and to $s = 2$ when σ_u is very large or, on the other hand, as friction becomes more or less important, respectively.

We may solve Eqs. (7.25) for Q'. We get

$$Q' = \frac{\zeta'^{\frac{s-1}{3}}}{(1+\zeta')^{\frac{s+1}{3}}} \tag{7.27}$$

Differentiating Eq. (7.27), we obtain

$$\frac{dQ'}{d\zeta'} = \frac{\frac{2}{3}\left(\frac{s-1}{2} - \zeta'\right)\zeta'^{\frac{s-4}{3}}}{(1+\zeta')^{\frac{s+4}{3}}} \tag{7.28}$$

so that Q' has a maximum, Q_c', when

$$\zeta_c' = \frac{s-1}{2} \tag{7.29}$$

The corresponding maximum value of Q is Q_c. Notice, also, that

$$\zeta'^{\frac{1}{3}} dQ' = d\xi' \tag{7.30}$$

so that ξ' and Q' increase or decrease together. This simply means that the flux in the upper level increases seaward, as is obvious for physical considerations.

Since $\mathcal{E}$ is a maximum when Q is a maximum, the flux may increase to the maximum as we move seaward but if this happens the estuary of constant width must then end.

It is enlightening to compute the Froude number F at ζ_c'. A convenient definition is

$$F^2 = \frac{\overline{u^2}}{D\Delta b} \tag{7.31}$$

This yields

$$F^2 = \gamma \frac{\bar{u}^2}{D\Delta b} = \frac{m}{\zeta} \tag{7.32}$$

Using (7.24) and (7.29), we get $F_c^2 = 1$, so that the maximum flux Q_c corresponds to a point of critical flow with supercritical flow for $\zeta' < \zeta_c'$ and subcritical flow for $\zeta' > \zeta_c'$. We may compare this to a theory by Stommel (1951) which led to the differential equation in Eq. (7.19) with $\lambda = 1$ and with the frictional term missing. He obtained

$$\frac{\eta}{Q}\frac{dQ}{d\eta} = \frac{1-F^2}{2(\frac{1}{4}-F^2)} \tag{7.33}$$

Stommel's theory was incomplete and he could not solve for fluxes and interface depths as functions of distance along the estuary.

From Eq. (7.25) we get

$$\frac{d\eta'}{d\zeta'} = \frac{\frac{1}{3}\zeta'^{\frac{s-3}{3}}(s-\zeta')}{(1+\zeta')^{\frac{s+4}{3}}} \tag{7.34}$$

Let us now consider the general properties of the solution. If we increase ζ' from $\zeta_c' = (s-1)/2$ (corresponding to subcritical flow), $s-\zeta'$ is positive at first and η' increases. It reaches a maximum at $\zeta' = s$ and then decreases as ζ' gets larger. Since Q' is decreasing, Eq. (7.30) shows that $\mathcal{E}'$ is decreasing so that we are moving toward the head of the estuary. On the other hand, if we decrease ζ' from ζ_c' (corresponding to supercritical flow), we find that η' decreases mono-

tonically. Again ξ' decreases so that we are again moving toward the head of the estuary. Thus, two distinct solutions are possible, but the second corresponds to high velocities in excess of a meter per second or more at the head of the estuary and elsewhere and seems unlikely to occur. It also involves a decrease of velocity and increase of elevation of the free surface toward the mouth and both are contrary to observations (Gade, 1970). Consequently, we adopt the solution, $\zeta' > \zeta'_c$, for subcritical flow.

The remaining problem concerns conditions at the mouth of the estuary. Let us assume that the estuary has a uniform width from the mouth to the head but at the mouth the width suddenly increases rapidly. The arguments leading to Eqs. (7.14)-(7.16) permit a variable width. Accordingly, let us derive two equations from Eqs. (7.15) and (7.16) yielding the rate of change of η and of $F^2 = mQ^3/\eta^3\lambda^2$ along the channel. We get

$$\frac{d\eta}{d\xi} = \frac{1}{1-F^2}\left\{\frac{2K_n m\lambda}{\gamma}\left(\frac{1}{4} - \frac{KF^2}{2mK_n\lambda} - F^2\right) + \frac{\eta F^2}{\lambda}\frac{d\lambda}{d\xi}\right\} \tag{7.35}$$

$$\frac{dF^2}{d\xi} = \frac{3F^2 K_n m\lambda}{\gamma\eta(1-F^2)}\left[F^2 + \frac{1}{2} + \frac{KF^2}{mK_n\lambda}\right] - \frac{F^2(F^2+2)}{\lambda(1-F^2)}\frac{d\lambda}{d\xi} \tag{7.36}$$

Let us now investigate all possibilities, shown in Fig. 7.2, for the location of the mouth of the estuary.

(a) The estuary ends at or before the section of maximum depth of the upper layer (point I or J).

In this case $1 - F^2 > 0$ and the quantity in curly brackets in Eq. (7.35) is positive to the left of I or J so that η is increasing with ξ. Eq. (7.36) reveals that F^2 is increasing but is considerably less than one. Just past point I or J, where λ is still close to one but $d\lambda/d\xi$ is very large, the last term in curly brackets in Eq. (7.35) will quickly dominate and η will increase even more rapidly. At

the same time, the last negative term in Eq. (7.36) will dominate and F^2 will start decreasing. If we now regard as physically necessary that η should decrease past the mouth as the mass of brackish water spreads in all directions, this case is impossible.

(b) The estuary ends after the section of maximum depth of the upper layer but not close to the section at which $F^2 = 1$.

In this case, η is decreasing just to the left of point K and F^2 is somewhat smaller than one and increasing. Just past K, however, the last term in curly brackets in Eq. (7.35) quickly dominates and η will reach a minimum and then increase. Also, the last negative term in Eq. (7.36) begins to dominate and F^2 begins to decrease. Again it is not possible for η to decrease past the mouth and this case is also impossible.

(c) The estuary ends just before the section at which $F^2 = 1$.

In this case, η is decreasing to the left of point L and F^2 is very close to one. Then, if $d\eta/d\xi$ remains finite, the quantity in curly brackets in Eq. (7.35) falls to zero at a section just past point L, F^2 passes through the critical value and $1 - F^2$ becomes negative. After this, the last term in curly brackets in Eq. (7.35) dominates and η continues to decrease. Eq. (7.36) shows that F^2 also continues to increase. This behavior is entirely reasonable and we, therefore, accept the point L as the end of the estuary. It is convenient to take this section as the origin of our coordinate system so that $\xi = \xi' = 0$ there and in Eqs. (7.23)-(7.26) Q_* and Q'_* may be replaced by Q_c and Q'_c.

7.3 Discussion.

We see from the theory that $\eta' = g(\xi', s)$ or, from Eq. (7.24), $C\eta Q'_h = g(\xi', s)$.

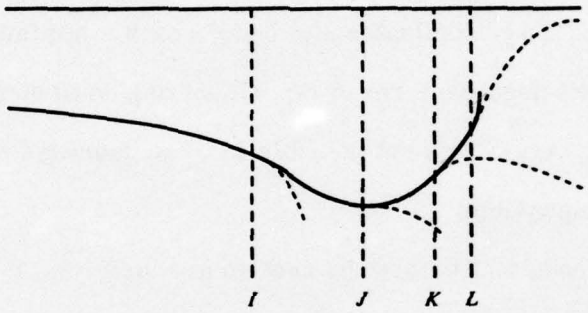

Fig. 7.2 Behavior of interface near mouth.

Also $Q' = f(\xi', s)$. We obtain then $Q_h' = f(\xi_h', s)$, $Q_c' = f(0, s)$, and

$$C\eta_h = \frac{g(\xi_h', s)}{f(\xi_h', s)} \ , \ Q_c = \frac{f(0, s)}{f(\xi_h', s)}$$

where ξ_h' is the value of ξ' at the head of the estuary where $|x| = L$. Computations for $s = 2$ and $s = 1.0036$ are shown in Figs. 7.3 and 7.4. They reveal that the maximum flux and the depth of the interface at the head increase monotonically with the length of the estuary. Other physical interpretations are obscured by the complicated scaling of the non-dimensional variables and we must assign values to the various constants to obtain useful interpretations of the theory.

We may refer to two extreme cases with respect to fresh-water influx, namely the inner Oslofjord (Gade, 1970) and the Knight Inlet (Pickard and Rodgers, 1959), for which we use $q_f = 60$ cm^2/sec and $2.3\ 10^3$ cm^2/sec respectively. It is important, of course, to estimate m in Eqs. (7.14), but this quantity is extremely sensitive to the value of σ_u. In either case, however, and in most estuaries, it seems likely that m is considerably less[1] than one. The quantity K_n has been estimated as $K_n \cong 0.1$. The constant K is uncertain but, as we have indicated, we will use $K = 1$. The estimates we have made so far mean that s is close to but a little larger than 1. The computations from the theory reveal little change in Q_c as $s \to 1$. At $mK_n CL\sigma_u/q_f\gamma = 3$, for example, Q_c increases by about 10% as s decreases from the rather large value of 1.2 to $s = 1.0036$. According to Fig. 7.3, we may write, approximately,

---

[1] In Knight Inlet, for example, we may take $\gamma = 1.3$, $\sigma_u = 5$ cm/sec, $b_o = 25$ cm/sec^2, $q_f = 2.3\ 10^3$ cm^2/sec. Then $m = 2.8\ 10^{-3}$. In the very different Oslofjord, we may take $\gamma = 1.3$, $\sigma_u = 1$ cm/sec, $b_o = 5$ cm/sec^{-2}, $q_f = 60$ cm^2/sec. Then $m = 4.3\ 10^{-3}$.

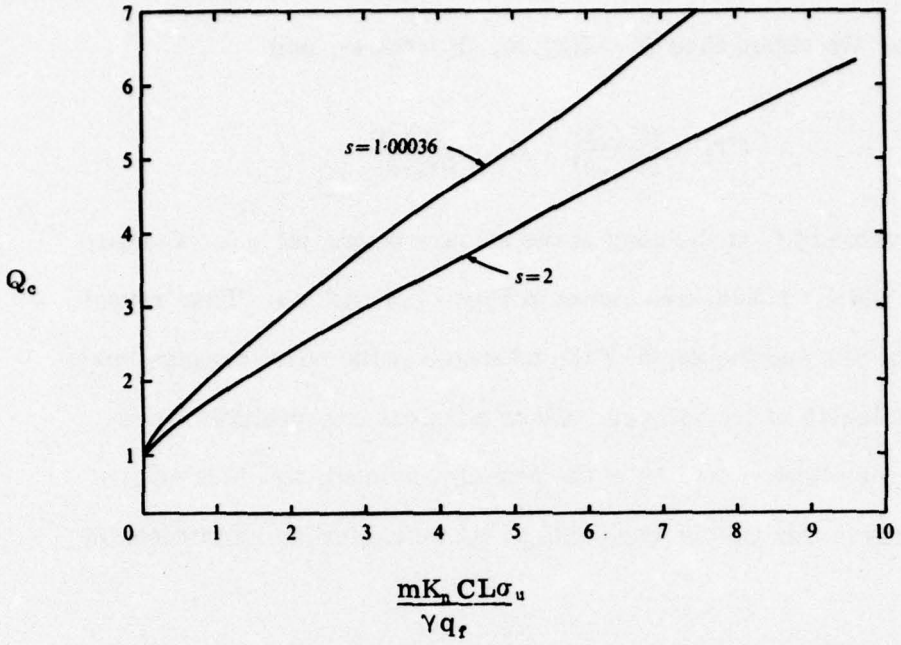

Fig. 7.3 Relationships between the mass flux in the upper layer and the estuary length

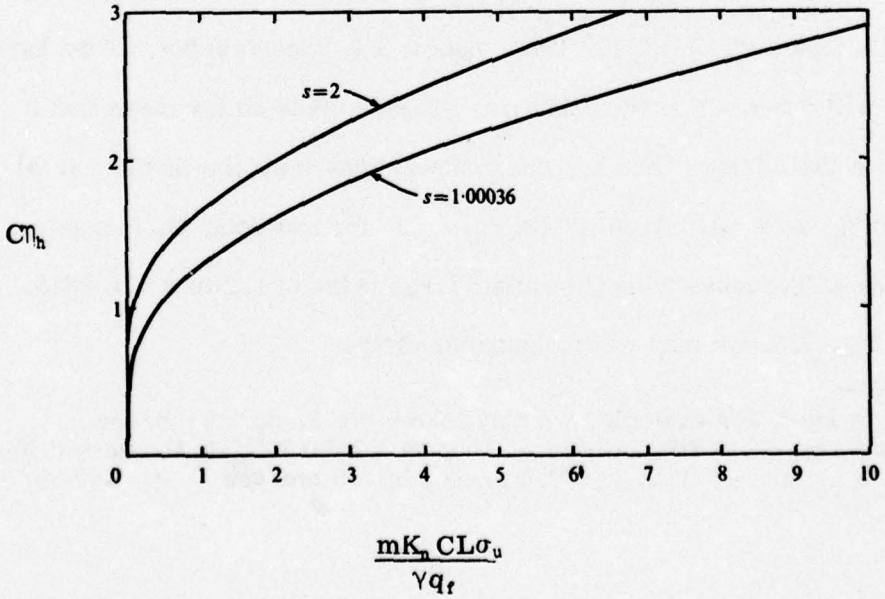

Fig. 7.4 Relationships between the halocline depth at the heac of the estuary and the estuary length.

$$Q_c \cong 1 + 0.9 \frac{mK_n CL\sigma_u}{\gamma q_f} \tag{7.37}$$

Our estimates lead to C = 0.37 and, with $\gamma = 1.3$, Eq. (7.37) may be written

$$Q_c \cong 1 + 0.033 \frac{L\sigma_u^4}{b_o q_f^2} \tag{7.38}$$

In the Oslofjord, with $L \cong 2.5\,10^6$ cm, $b_o = 5$ cm/sec^2 and $Q_c \cong 3.2$ (Gade, 1970), we estimate $\sigma_u \cong 0.83$ cm/sec. In the Knight Inlet, Q_c is quite uncertain, but the data suggests a value of perhaps 4. Using $L \cong 1.1\,10^7$ cm, $b_o \cong 25$ cm/sec^2, we obtain $\sigma_u = 5.7$ cm/sec.

Computations for various values of s near 1 reveal little variation of $C\eta_h$ with s for all but very short estuaries. A rough relationship is

$$C\eta_h \cong 1 + 0.25 \frac{mK_n CL\sigma_u}{\gamma q_f} \tag{7.39}$$

or, approximately,

$$D_h \cong 2.7 \frac{q_f}{\sigma_u} + 0.025\, L \frac{\sigma_u^3}{b_o q_f} \tag{7.40}$$

Computations in Fig. 7.3 and 7.4 yield $C\eta_h = 1.7$ and 1.9, respectively, for the Oslofjord and the Knight Inlet. We get approximately $D_h = 3.3$m for the Oslofjord and 21 m for the Knight Inlet. The first is a considerable underestimate for the Oslofjord but the second is close to observations in the Knight Inlet. The comparisons suggest that the model of this paper may contain the basic physical mechanisms of the Knight Inlet but probably differs fundamentally from the Oslofjord. This is not surprising. The former has a geometry similar to the model whereas the latter is very different. For example, the Oslofjord has a shallow sill depth which forms a considerable barrier for the influx of salt water, whereas the sill depths of the Knight Inlet are well below the halocline. There is, moreover,

the observed basic difference in the horizontal density variation. This is similar to the model in the Knight Inlet but is virtually absent in the Oslofjord, so that the basic driving mechanism of the present model is absent in the latter. As we discuss in Section 8, the Oslofjord appears to be influenced primarily by the density distribution in the waters outside of the fjord.

Notice that if we consider D_h as a function of q_f, Eq. (7.40) shows that the halocline depth is a minimum for a certain value of q_f and large for both small and large values of the fresh-water discharge. This is the same as the behavior discussed in Section 6.

An interesting feature of the theory is the slope of the free surface. As we have noted, the surface slopes downward toward the mouth in subcritical flow and Eq. (7.4) yields for the total drop ΔH,

$$\Delta H = \frac{q_f b_0}{\sigma_u g C} \Delta\zeta'^{\frac{1}{3}} \tag{7.41}$$

For the Knight Inlet, for example, $\Delta\zeta'^{\frac{1}{3}} \simeq 2$, and we get $\Delta H \simeq 55$ cm. This seems rather large but values of 10-15 cm in shorter Norwegian fjords have been found by Gade (personal communication). Notice that the commonly used argument that the free surface must slope downward toward the mouth (Gade, 1974) implicitly assumes subcritical flow. We have not discussed the supercritical case in which the free surface slopes upward toward the sea, but it is possible that some estuaries have this character.

The calculated drop of surface level for the Knight Inlet represents a potential energy far in excess of the observed or theoretical kinetic energies and we conclude that friction dominates the flow. This is probably true of most fjord-type estuaries. We also deduce the dominate effect of friction from the

fact that s tends to be very close to 1. As we see in Eq. (7.20) this corresponds to large values of the drag coefficient K. Indeed, the ratio of inertial forces to pressure or frictional forces is proportional to s-1.

7.3 Estuary of Arbitrary Width - Integration Procedure.

We may outline the procedure for finding the solution for an estuary of arbitrary shape. We first notice that Eqs. (7.35) and (7.36) are invariant for transformations $\eta = \alpha\eta^*$, $\xi = \alpha\xi^*$. Using $\lambda = f(\xi^*)$, we may write

$$f(1-F^2)\frac{d\eta^*}{d\xi^*} = \frac{2K_n m}{\gamma} f^2(\tfrac{1}{4}-F^2) - \frac{K}{\gamma} fF^2 + \eta^* F^2 \frac{df}{d\xi^*} \tag{7.42}$$

$$\eta^*(1-F^2)f\frac{dF^2}{d\xi^*} = \frac{3K_n m}{\gamma} F^2 f^2 (F^2+\tfrac{1}{2}) + \frac{3F^4 Kf}{\gamma} - F^2(F^2+2)\eta^* \frac{df}{d\xi^*} \tag{7.43}$$

Let us investigate the solution in the region just past the mouth ($\xi^* = 0$) where, by assumption, the width of the estuary increases linearly. At $\xi^* = a$, the flow becomes critical. Then if $\zeta^* = \xi^* - a$ and λ_m is the value of λ at $\xi^* = 0$,

$$\eta^* = \eta_c^* + b_1\zeta^* + \ldots, \quad F^2 = 1 + a_1\zeta^* + \ldots, \quad f = \lambda_m + c_1 a + c_1\zeta^* \tag{7.44}$$

Substituting (7.44) into (7.42) and (7.43) and equating coefficients of ζ^* we obtain to zero order two identical equations. This may be used to solve for $\lambda_m + c_1 a$:

$$\lambda_m + c_1 a = \frac{-\frac{K}{\gamma} + \sqrt{\frac{K^2}{\gamma^2} + \frac{6c_1 K_n m \eta_c^*}{\gamma}}}{3K_n m/\gamma} \tag{7.45}$$

The other two equations obtained from equating coefficients of ζ^* may be written

$$A_1 b_1 + B_1 \eta_c^* = E_1 \tag{7.46}$$

$$A_2 b_1 + B_2 \eta_c^* = E_2 \tag{7.47}$$

where

$$A_1 = a_1(\lambda_m + c_1 a) + c_1, \quad B_1 = c_1 a_1, \quad A_2 = -3c_1, \quad B_2 = a_1^2(\lambda_m + c_1 a) - 4c_1 a_1 \tag{7.48}$$

$$E_1 = + \frac{2K_n m}{\gamma}\left[\frac{3}{2}c_1(\lambda_m + c_1 a) + a_1(\lambda_m + c_1 a)^2\right] + \frac{K}{\gamma}\left[a_1(\lambda_m + c_1 a) + c_1\right] \tag{7.49}$$

$$E_2 = - \frac{3K_n m}{\gamma}\left[\frac{5}{2}a_1(\lambda_m + c_1 a)^2 + 3c_1(\lambda_m + c_1 a)\right] - \frac{3K}{\gamma}\left[2a_1(\lambda_m + c_1 a) + c_1\right] \tag{7.50}$$

Thus

$$b_1 = (E_1 B_2 - E_2 B_1)/(A_1 B_2 - A_2 B_1) \tag{7.51}$$

$$\eta_c^* = (A_1 E_2 - A_2 E_1)/(A_1 B_2 - A_2 B_1) \tag{7.52}$$

The integration may then proceed as follows. We specify λ_m and c_1 and the constants K_n, m, γ. We also specify a_1. This permits calculation of b_1 and η_c^* from (7.51) and (7.52), and $\lambda_m + c_1 a$ from (7.45). We may then compute η^* and F^2 from (7.44) for say $\xi^* = 0$, and $\xi^* = -\Delta\xi^*$. We may then use the finite difference forms of (7.42) and (7.43) to compute F^2 and η^* at subsequent grid points until $\lambda = 1$. This corresponds to the head of the estuary, where $F^2 = F_h^2$, $Q = 1$, $\eta_h = \eta_h^* \alpha$. Then we have

$$\alpha^3 = \frac{m}{F_h^2 \eta_h^{*3}} \tag{7.53}$$

and we have a solution for an estuary of width,

$$\lambda = f\left(\frac{\xi}{\alpha}\right) \tag{7.54}$$

8. Three-Layer Circulations in Estuaries and Harbors.

A number of writers beginning, apparently, with Hachey (1934) have remarked that if a density variation with depth exists in the water outside of an embayment and if there is a source of mixing in the embayment from tides and wind, there will

fact that s tends to be very close to 1. As we see in Eq. (7.20) this corresponds to large values of the drag coefficient K. Indeed, the ratio of inertial forces to pressure or frictional forces is proportional to s-1.

7.3 Estuary of Arbitrary Width - Integration Procedure.

We may outline the procedure for finding the solution for an estuary of arbitrary shape. We first notice that Eqs. (7.35) and (7.36) are invariant for transformations $\eta = \alpha\eta^*$, $\xi = \alpha\xi^*$. Using $\lambda = f(\xi^*)$, we may write

$$f(1-F^2)\frac{d\eta^*}{d\xi^*} = \frac{2K_n m}{\gamma} f^2\left(\tfrac{1}{4}-F^2\right) - \frac{K}{\gamma} f F^2 + \eta^* F^2 \frac{df}{d\xi^*} \tag{7.42}$$

$$\eta^*(1-F^2) f \frac{dF^2}{d\xi^*} = \frac{3K_n m}{\gamma} F^2 f^2 \left(F^2+\tfrac{1}{2}\right) + \frac{3F^4 K f}{\gamma} - F^2(F^2+2)\eta^* \frac{df}{d\xi^*} \tag{7.43}$$

Let us investigate the solution in the region just past the mouth ($\xi^* = 0$) where, by assumption, the width of the estuary increases linearly. At $\xi^* = a$, the flow becomes critical. Then if $\zeta^* = \xi^* - a$ and λ_m is the value of λ at $\xi^* = 0$,

$$\eta^* = \eta_c^* + b_1\zeta^* + \ldots, \quad F^2 = 1 + a_1\zeta^* + \ldots, \quad f = \lambda_m + c_1 a + c_1\zeta^* \tag{7.44}$$

Substituting (7.44) into (7.42) and (7.43) and equating coefficients of ζ^* we obtain to zero order two identical equations. This may be used to solve for $\lambda_m + c_1 a$:

$$\lambda_m + c_1 a = \frac{-\frac{K}{\gamma} + \sqrt{\frac{K^2}{\gamma^2} + \frac{6c_1 K_n m \eta_c^*}{\gamma}}}{3K_n m/\gamma} \tag{7.45}$$

The other two equations obtained from equating coefficients of ζ^* may be written

$$A_1 b_1 + B_1 \eta_c^* = E_1 \tag{7.46}$$

$$A_2 b_1 + B_2 \eta_c^* = E_2 \tag{7.47}$$

be a tendency for a density distribution as shown in Fig. 8.1 and a resulting three-layer circulation from the density-pressure effect even in the absence of a fresh-water influx. Stroup, Pritchard and Carpenter (1961) have calculated that this type of circulation is dominant as a flushing mechanism for Baltimore Harbor in the Chesapeake Bay. Here the less salty water in the upper layer outside of the harbor originates from the fresh water discharge of the Susquehanna River at the head of the Chesapeake Bay. It has also been suggested that the outside density distribution is important for the circulations in the Oslofjord in Norway (Gade, 1970) and in the Gullmarfjord on the west coast of Sweden (Rydberg, 1975). Rydberg observed inflow in the layer below the halocline at the sill and inferred from considerations of conservation of salt that there must be an influx of lower salinity water somewhere in the upper level. Conservation of mass requires an efflux of water at some intermediate level. The lower salinity water outside of the Oslofjord and the Gullmarfjord originates as the brackish water flowing out of the Danish sounds from the Baltic Sea. The three-layer type of circulation has also been discussed by Hansen and Rattray (1972).

A simple laboratory model of a three-layer circulation was constructed by Hachey (1934). It is shown schematically in Fig. 8.2. A long channel contains, initially, two layers of water of different density. At one end of the channel a cylinder at the interface is rotated as shown to provide a source of mixing. The resulting pressure-density distribution produces the three-layer circulation in the figure.

The simplest model of the basic phenomenon of this section is one in which

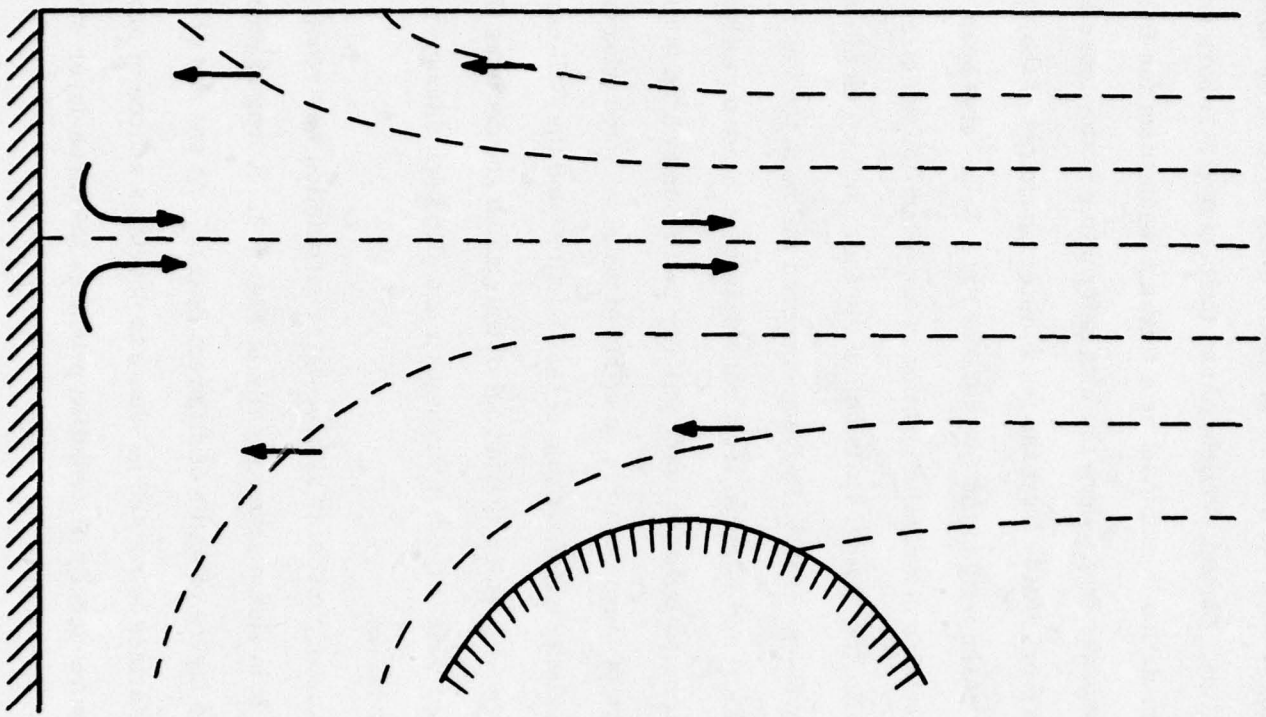

Fig. 8.1 Schematic density distribution in an embayment producing three-layer circulation

there is an ocean, infinite laterally, composed of two layers with buoyancy difference Δb_o and with an upper layer of depth h. These are the conditions outside of an embayment of arbitrary geometry specified by lengths $L_1, L_2, \ldots$. The fresh water influx is zero. There is some source of mixing in the estuary. The nature of the mixing is not important for the ultimate argument, I think, but for simplicity let us consider a mechanism similar to the one we use in the experiment discussed at the end of this section, namely a rotating propellor located at depth h of angular speed ω and geometry specified by the lengths $a_1, a_2, \ldots$. This mixing will result in an efflux in the vicinity of the depth h of magnitude q_1. Dimensional analysis yields

$$\frac{q_1}{h^{\frac{5}{2}}(\Delta b_o)^{\frac{1}{2}}} = f\left(\frac{h\omega^2}{\Delta b_o}, \frac{L_1}{h}, \frac{L_2}{h}, \ldots, \frac{a_1}{h}, \frac{a_2}{h} \ldots\right) \tag{8.1}$$

Now let ω increase from a low value. q_1 increases with ω. At some value of ω the estuary becomes thoroughly mixed and any further increase in ω will have no effect on the density of the fluid in the estuary and, therefore, no effect on q_1. For higher ω, we have $\partial q_1 / \partial \omega = 0$. Therefore, Eq. (8.1) becomes independent of ω, i.e.,

$$\frac{q_1}{h^{\frac{5}{2}}(\Delta b_o)^{\frac{1}{2}}} = f\left(\frac{L_1}{h}, \frac{L_2}{h}, \ldots, \frac{a_1}{h}, \frac{a_2}{h}, \ldots\right) \tag{8.2}$$

This tells us nothing about the variation of q_1 with any of the lengths of the problem but does indicate that the efflux is directly proportional to the square-root of the density difference between the two fluids when the estuary is thoroughly mixed. We may extend this to the more realistic case of an outside linear density gradient and find that q_1 is proportional to the square root of the density gradient.

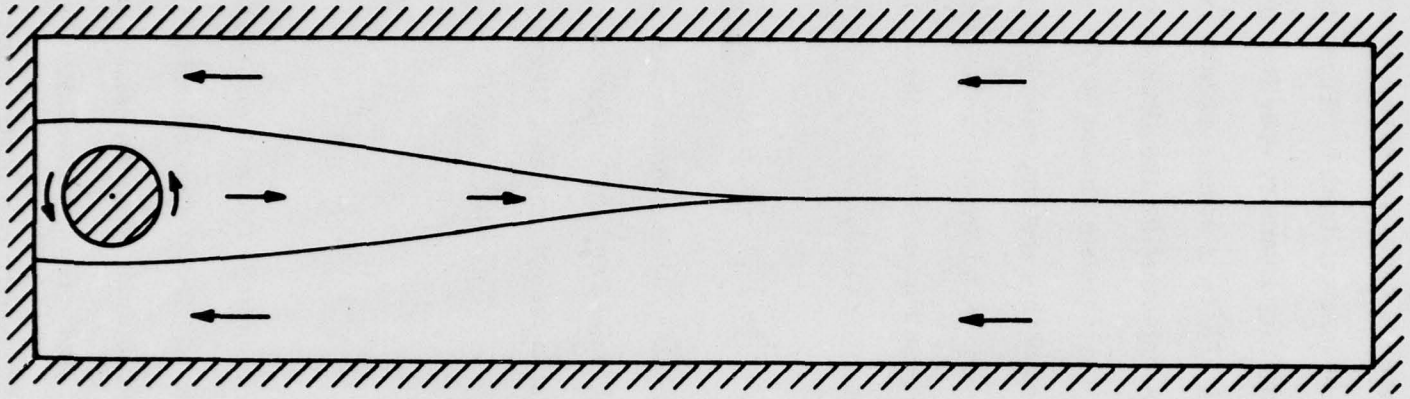

Fig. 8.2 Hachey's experiment.

Let us make a detailed investigation of the three-layer circulation (Long, 1977). The model is shown schematically in Fig. 8.3. The estuary-harbor is on the left of the figure. We assume that the width of the channel B, located between the estuary-harbor and the outside water, is independent of z. The bottom of the channel and of the two bodies of water has an equation $z = \zeta(x)$ with $z = 0$ chosen at a depth H below the level of the outside body of water. The equation of the free surface is $z = H + \Delta H$ where ΔH is small and only important with respect to the pressure distribution. Outside of the estuary-harbor there is a two-layer system with an upper layer of thickness h. The upper layer has a salinity S_0 and the lower layer has a salinity S_2. The water in the estuary is thoroughly mixed and has a salinity S_1. The corresponding densities are ρ_0, ρ_1 and ρ_2. Later we confine attention to a model with a uniform depth H everywhere and a zero fresh-water influx. Here the fresh-water influx R is finite and if the depth is variable we require that it be a minimum at the section of minimum width W. The fluxes of water of salinity S_0, S_1 and S_2 are q_0, q_1 and q_2, respectively. The lower interface has an equation $z = z_2$ and the upper interface an equation $z = z_1$ so that the thicknesses of the three layers are $(z_2 - \zeta)$, $(z_1 - z_2)$ and $(H - z_1)$, respectively, if we neglect the small quantity ΔH except as it influences the pressure distribution. At the constriction the thicknesses of the layers are $\eta_2 H$, $(1 - \eta_0 - \eta_2)H$, and $\eta_0 H$, respectively.

Using the hydrostatic approximation, the three Bernoulli equations are

$$\rho_0 g(H + \Delta H) + \frac{\rho_0 q_0^2}{2B^2 (H - z_1)^2} = \rho_0 g H \tag{8.3}$$

$$(\rho_1 - \rho_0) g z_1 + \rho_0 g(H + \Delta H) + \frac{\rho_1 q_1^2}{2B^2 (z_1 - z_2)^2} = \text{constant} \tag{8.4}$$

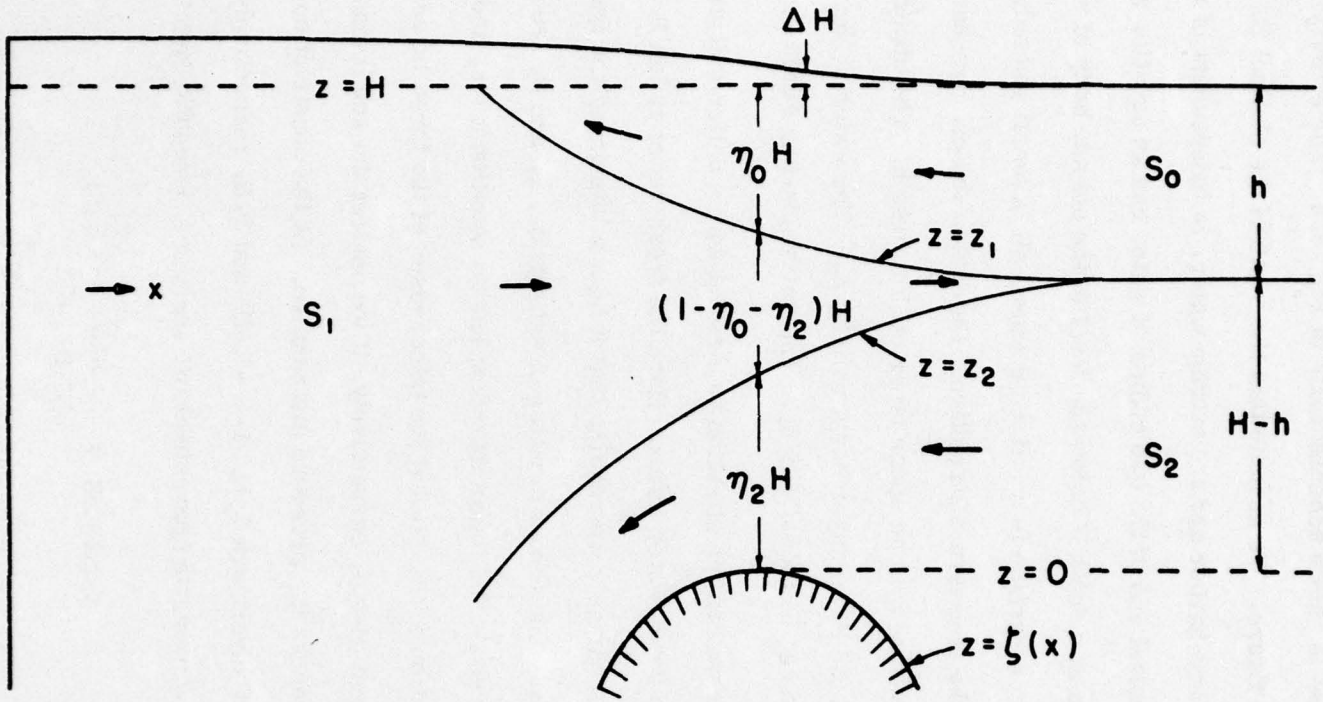

Fig. 8.3 Mouth of estuary-harbor

$$(\rho_2-\rho_1)gz_2 + (\rho_1-\rho_0)gz_1 + \rho_0 g(H+\Delta H) + \frac{\rho_2 q_2^2}{2B^2(z_2-\zeta)^2} = (\rho_2-\rho_0)g(H-h) + \rho_0 gH \tag{8.5}$$

With the Boussinesq approximation, these become

$$g\Delta H + \frac{q_0^2}{2B^2(H-z_1)^2} = 0 \tag{8.6}$$

$$(\Delta b_0-\Delta b_1)z_1 + g\Delta H + \frac{q_1^2}{2B^2(z_1-z_2)^2} = \text{constant} \tag{8.7}$$

$$z_2\Delta b_1 + (\Delta b_0-\Delta b_1)z_1 + g\Delta H + \frac{q_2^2}{2B^2(z_2-\zeta)^2} = \Delta b_0(H-h) \tag{8.8}$$

where we have used the definitions

$$\Delta b_1 = g\frac{(\rho_2-\rho_1)}{\rho_2}\ ,\ \Delta b_0 = g\frac{\rho_2-\rho_0}{\rho_2} \tag{8.9}$$

Let us now differentiate Eqs. (8.6)-(8.8) with respect to x, evaluating at the section of minimum depth and width where $\partial B/\partial x = 0$, $\partial\zeta/\partial x = 0$, $B = W$, $H-z_1 = \eta_0 H$, $z_1-z_2 = (1-\eta_0-\eta_2)H$, $z_2-\zeta = \eta_2 H$. We get

$$\frac{\partial}{\partial x}(g\Delta H) + \frac{q_0^2}{W^2\eta_0^3H^3}\frac{\partial z_1}{\partial x} = 0 \tag{8.10}$$

$$\frac{\partial}{\partial x}(g\Delta H) + (\Delta b_0-\Delta b_1)\frac{\partial z_1}{\partial x} - \frac{q_1^2}{W^2(1-\eta_0-\eta_2)^3H^3}\left(\frac{\partial z_1}{\partial x}-\frac{\partial z_2}{\partial x}\right) = 0 \tag{8.11}$$

$$\frac{\partial}{\partial x}(g\Delta H) + \Delta b_1\frac{\partial z_2}{\partial x} + (\Delta b_0-\Delta b_1)\frac{\partial z_1}{\partial x} - \frac{q_2^2}{W^2\eta_2^3H^3}\frac{\partial z_2}{\partial x} = 0 \tag{8.12}$$

We may assume (Long, 1976) that the interfaces and free surface do not have a zero slope at the constriction so that the determinant of Eqs. (8.10)-(8.12) is zero. We obtain the critical condition

$$\left[(\Delta b_0-\Delta b_1)-\frac{q_1^2}{W^2(1-\eta_0-\eta_2)^3H^3}\right]\left[\Delta b_1-\frac{q_2^2}{W^2\eta_2^3H^3}\right]-(\Delta b_0-\Delta b_1)\frac{q_1^2}{W^2(1-\eta_b-\eta_2)^3H^3}$$

$$-\frac{q_0^2}{W^2\eta_b^3H^3}\left[\Delta b_1-\frac{q_2^2}{W^2\eta_2^3H^3}-\frac{q_1^2}{W^2(1-\eta_0-\eta_2)^3H^3}\right]=0 \tag{8.13}$$

The equations for conservation of volume and salt are

$$R+q_0+q_2=q_1 \tag{8.14}$$

$$q_0S_0+q_2S_2=q_1S_1 \tag{8.15}$$

If we use a linear relationship between density and salinity, we obtain

$$q_0=\frac{q_1}{s}-\frac{R}{r} \tag{8.16}$$

$$q_2=\frac{q_1(s-1)}{s}-\frac{R(r-1)}{r} \tag{8.17}$$

where $s=\Delta b_0/\Delta b_1$, $r=\Delta b_0/b_2$ and where b_2 is the buoyancy of water of salinity S_2. With the following definitions,

$$Q_1^2=\frac{q_1^2}{W^2H^3\Delta b_0},\quad Q_0^2=\frac{q_0^2}{W^2H^3\Delta b_0},\quad \beta=\frac{h}{H}$$

$$Q_2^2=\frac{q_2^2}{W^2H^3\Delta b_0},\quad Q_f^2=\frac{R^2}{W^2H^3\Delta b_0}$$

Eqs. (8.16) and (8.17) become

$$Q_0=\frac{Q_1}{s}-\frac{Q_f}{r},\quad Q_2=\frac{Q_1(s-1)}{s}-\frac{Q_f(r-1)}{r} \tag{8.18}$$

Eq. (8.13) and a combination of Eqs. (8.6) and (8.8) leads to

$$\left\{(s-1) - \frac{Q_1^2 s}{(1-\eta_0-\eta_2)^3}\right\}\left\{1 - \frac{[Q_1(s-1)-Q_f\frac{s}{r}(r-1)]^2}{\eta_2^3 s}\right\} - \frac{s(s-1)Q_1^2}{(1-\eta_0-\eta_2)^3}$$

$$- \frac{(Q_1 - \frac{s}{r}Q_f)^2}{\eta_0^3 s}\left\{1 - \frac{[Q_1(s-1)-Q_f\frac{s}{r}(r-1)]^2}{\eta_2^3 s} - \frac{Q_1^2 s}{(1-\eta_0-\eta_2)^3}\right\} = 0 \qquad (8.19)$$

$$\eta_2 + (s-1)(1-\eta_0) - \frac{(Q_1 - \frac{s}{r}Q_f)^2}{2\eta_0^2 s} + \frac{[Q_1(s-1)-Q_f\frac{s}{r}(r-1)]^2}{2\eta_2^2 s} - s(1-\beta) = 0 \qquad (8.20)$$

Eqs. (8.19) and (8.20) may be put in the following convenient forms:

$$f_1(Q_1, \eta_0, \eta_2, s; r, \beta, Q_f) = 2\eta_0^2\eta_2^3 s + 2\eta_0^2\eta_2^2 s(s-1)(1-\eta_0) - \eta_2^2[Q_1 - \frac{s}{r}Q_f]^2$$

$$+ \eta_0^2[Q_1(s-1)-Q_f\frac{s}{r}(r-1)]^2 - 2s^2\eta_0^2\eta_2^2(1-\beta) = 0 \qquad (8.21)$$

$$f_2(Q_1, \eta_0, \eta_2, s; r, \beta, Q_f) = \{(s-1)(1-\eta_0-\eta_2)^3 - Q_1^2 s\}\{\eta_2^3 s - [Q_1(s-1)-Q_f\frac{s}{r}(r-1)]^2\}\eta_0^3 s$$

$$-(s-1)Q_1^2\eta_0^3\eta_2^3 s^3 - (Q_1 - \frac{s}{r}Q_f)^2(1-\eta_0-\eta_2)^3\eta_2^3 s + Q_1^2(Q_1 - \frac{s}{r}Q_f)^2 s^2\eta_2^3 \qquad (8.22)$$

$$+ (Q_1 - \frac{s}{r}Q_f)^2[Q_1(s-1)-Q_f\frac{s}{r}(r-1)]^2(1-\eta_0-\eta_2)^3 = 0$$

Let us now consider r, β and Q_f fixed in the functions in Eqs. (8.21) and (8.22), i.e., we write

$$f_1(Q_1, \eta_0, \eta_2, s) = 0 \qquad (8.23)$$

$$f_2(Q_1, \eta_0, \eta_2, s) = 0 \qquad (8.24)$$

Solving Eq. (8.23) for s, we get

$$s = m(Q_1, \eta_0, \eta_2) \tag{8.25}$$

Substituting (8.25) into (8.24) we get

$$f_2 [Q_1, \eta_0, \eta_2, m(Q_1, \eta_0, \eta_2)] = P(Q_1, \eta_0, \eta_2) = 0 \tag{8.26}$$

Thus

$$Q_1 = \chi(\eta_0, \eta_2), \quad s = \Lambda(\eta_0, \eta_2) \tag{8.27}$$

We assume that the non-dimensional flux Q_1 increases as the mixing increases. When the estuary-harbor is thoroughly mixed, any further increase in the mixing will not change Q_1. As in earlier arguments, we assume that this occurs when Q_1 is a maximum, now with respect to the variation of two quantities η_0 and η_2 in the equation, $Q_1 = \chi(\eta_0, \eta_2)$. Thus we require for an overmixed estuary

$$\left.\frac{\partial \chi}{\partial \eta_0}\right|_{\eta_2} = 0, \quad \left.\frac{\partial \chi}{\partial \eta_2}\right|_{\eta_0} = 0 \tag{8.28}$$

where to make matters perfectly clear, we use subscripts to indicate the variables held fixed in the partial differentiation. To find Eqs. (8.28) in a useful form, let us differentiate (8.23) and (8.24)

$$\left(\frac{\partial f_1}{\partial Q_1}\right)_{\eta_0, \eta_2, s} \left(\frac{\partial \chi}{\partial \eta_0}\right)_{\eta_2} + \left(\frac{\partial f_1}{\partial \eta_0}\right)_{Q_1, \eta_2, s} + \left(\frac{\partial f_1}{\partial s}\right)_{Q_1, \eta_0, \eta_2} \left(\frac{\partial \Lambda}{\partial \eta_0}\right)_{\eta_2} = 0 \tag{8.29}$$

$$\left(\frac{\partial f_1}{\partial Q_1}\right)_{\eta_0, \eta_2, s} \left(\frac{\partial \chi}{\partial \eta_2}\right)_{\eta_0} + \left(\frac{\partial f_1}{\partial \eta_2}\right)_{Q_1, \eta_0, s} + \left(\frac{\partial f_1}{\partial s}\right)_{Q_1, \eta_0, \eta_2} \left(\frac{\partial \Lambda}{\partial \eta_2}\right)_{\eta_0} = 0 \tag{8.30}$$

$$\left(\frac{\partial f_2}{\partial Q_1}\right)_{\eta_0, \eta_2, s} \left(\frac{\partial \chi}{\partial \eta_0}\right)_{\eta_2} + \left(\frac{\partial f_2}{\partial \eta_0}\right)_{Q_1, \eta_2, s} + \left(\frac{\partial f_2}{\partial s}\right)_{Q_1, \eta_0, \eta_2} \left(\frac{\partial \Lambda}{\partial \eta_0}\right)_{\eta_2} = 0 \tag{8.31}$$

$$\left(\frac{\partial f_2}{\partial Q_1}\right)_{\eta_0, \eta_2, s} \left(\frac{\partial \chi}{\partial \eta_2}\right)_{\eta_0} + \left(\frac{\partial f_2}{\partial \eta_2}\right)_{Q_1, \eta_0, s} + \left(\frac{\partial f_2}{\partial s}\right)_{Q_1, \eta_0, \eta_2} \left(\frac{\partial \Lambda}{\partial \eta_2}\right)_{\eta_0} = 0 \tag{8.32}$$

Using (8.28) and eliminating $\partial\Lambda/\partial\eta_0$ and $\partial\Lambda/\partial\eta_2$, we obtain

$$\frac{\partial f_1}{\partial \eta_0}\frac{\partial f_2}{\partial s} = \frac{\partial f_2}{\partial \eta_0}\frac{\partial f_1}{\partial s} \tag{8.33}$$

$$\frac{\partial f_1}{\partial \eta_2}\frac{\partial f_2}{\partial s} = \frac{\partial f_2}{\partial \eta_2}\frac{\partial f_1}{\partial s} \tag{8.34}$$

where we now suppress the subscripts. Eqs. (8.33) and (8.34) together with Eqs. (8.21) and (8.22) are four equations in four unknowns, Q_1, η_0, η_2, $s(r, \beta, Q_f$ given) and the problem is determinate. The quantities in Eqs. (8.33) and (8.34) are

$$\frac{\partial f_1}{\partial \eta_0} = 4\eta_0\eta_2^3 s + 4\eta_0\eta_2^2 s(s-1)(1-\eta_0) - 2\eta_0^2\eta_2^2 s(s-1) + 2\eta_0\left[Q_1(s-1) - Q_f\frac{s}{r}(r-1)\right]^2 \tag{8.35}$$

$$-4s^2\eta_0\eta_2^2(1-\beta)$$

$$\frac{\partial f_1}{\partial \eta_2} = 6\eta_2^2\eta_0^2 s + 4\eta_0^2\eta_2 s(s-1)(1-\eta_0) - 2\eta_2\left(Q_1 - \frac{s}{r}Q_f\right)^2 - 4s^2\eta_0^2\eta_2(1-\beta) \tag{8.36}$$

$$\frac{\partial f_1}{\partial s} = 2\eta_0^2\eta_2^3 + 2\eta_0^2\eta_2^2(s-1)(1-\eta_0) + 2\eta_0^2\eta_2^2 s(1-\eta_0) + 2\eta_0^2\left[Q_1(s-1) - Q_f\frac{s}{r}(r-1)\right]\left[Q_1 - \frac{Q_f}{r}(r-1)\right] \tag{8.37}$$

$$+ \frac{2Q_f}{r}\left[Q_1 - \frac{s}{r}Q_f\right]\eta_2^2 - 4s\eta_0^2\eta_2^2(1-\beta)$$

$$\frac{\partial f_2}{\partial \eta_0} = -3(s-1)(1-\eta_0-\eta_2)^2\eta_0^3 s\left\{\eta_2^3 s - \left[Q_1(s-1) - Q_f\frac{s}{r}(r-1)\right]^3\right\} - 3(s-1)Q_1^2\eta_0^2\eta_2^3 s^3$$

$$+3\eta_0^2 s(s-1)(1-\eta_0-\eta_2)^3 - Q_1^2 s\left\{\eta_2^3 s - \left[Q_1(s-1) - Q_f\frac{s}{r}(r-1)\right]^2\right\} + 3\left(Q_1 - \frac{s}{r}Q_f\right)^2(1-\eta_0-\eta_2)^2\eta_2^3 s \tag{8.38}$$

$$-3(1-\eta_0-\eta_2)^2\left(Q_1 - \frac{s}{r}Q_f\right)^2\left[Q_1(s-1) - Q_f\frac{s}{r}(r-1)\right]^2$$

$$\frac{\partial f_2}{\partial \eta_2} = -3(s-1)(1-\eta_0-\eta_2)^2\eta_0^3 s\left[\eta_2^3 s-\left[Q_1(s-1)-Q_f\frac{s}{r}(r-1)\right]^2\right]+3\eta_2^2\eta_0^3 s^2\left[(s-1)(1-\eta_0-\eta_2)^3-Q_1^2 s\right]$$

$$-3\eta_2^2\eta_0^3(s-1)Q_1^2 s^3+3\left(Q_1-\frac{s}{r}Q_f\right)^2(1-\eta_0-\eta_2)^2\eta_2^3 s-3\eta_2^2 s(1-\eta_0-\eta_2)^3\left(Q_1-\frac{s}{r}Q_f\right)^2 \quad (8.39)$$

$$-3(1-\eta_0-\eta_2)^2\left(Q_1-\frac{s}{r}Q_f\right)^2\left[Q_1(s-1)-Q_f\frac{s}{r}(r-1)\right]^2+3Q_1^2 s^2\eta_2^2\left(Q_1-\frac{s}{r}Q_f\right)^2$$

$$\frac{\partial f_2}{\partial s} = (1-\eta_0-\eta_2)^3-Q_1^2\left[\eta_2^3 s-\left[Q_1(s-1)-Q_f\frac{s}{r}(r-1)\right]^2\right]\eta_0^3 s-(4s^3-3s^2)Q_1^2\eta_0^3\eta_2^3$$

$$+\eta_0^3\left[(s-1)(1-\eta_0-\eta_2)^3-Q_1^2 s\right]\left[\eta_2^3 s-\left[Q_1(s-1)-Q_f\frac{s}{r}(r-1)\right]^2\right]$$

$$+\eta_0^3 s\left[(s-1)(1-\eta_0-\eta_2)^3-Q_1^2 s\right]\left[\eta_2^3-2\left[Q_1(s-1)-Q_f\frac{s}{r}(r-1)\right]\left[Q_1-Q_f\frac{(r-1)}{r}\right]\right] \quad (8.40)$$

$$+2\frac{Q_f}{r}\left(Q_1-\frac{s}{r}Q_f\right)\eta_2^3 s(1-\eta_0-\eta_2)^3-\eta_2^3(1-\eta_0-\eta_2)^3\left(Q_1-\frac{s}{r}Q_f\right)^2$$

$$-2\frac{Q_f}{r}\left(Q_1-\frac{s}{r}Q_f\right)\left[Q_1(s-1)-Q_f\frac{s}{r}(r-1)\right]^2(1-\eta_0-\eta_2)^3-2Q_1^2\left(Q_1-\frac{s}{r}Q_f\right)\frac{Q_f}{r}s^2\eta_2^3$$

$$+2\left[Q_1(s-1)-Q_f\frac{s}{r}(r-1)\right]\left[Q_1-\frac{Q_f}{r}(r-1)\right]\left[Q_1-\frac{s}{r}Q_f\right]^2(1-\eta_0-\eta_2)^3+2Q_1^2 s\eta_2^3\left(Q_1-\frac{s}{r}Q_f\right)^2$$

The solution of the general problem involves the solution of the four complicated simultaneous algebraic equations and we will limit attention to the special case in the next section. We note, however, that for a zero fresh-water influx, the solution has the simple form $Q_1 = f(\beta)$ so that the discharge q_1 is proportional to the square root of the density difference between the two outside fluids as we found out from dimensional analysis.

Let us now consider the special case in which the whole system has a uniform depth H, the fresh-water flux is zero, and the two fluids outside of the harbor have equal thicknesses. Then $\beta = \frac{1}{2}$ and from symmetry $s = 2$ and $\eta_2 = \eta_0$. Eq. (8.21) becomes an identity and Eq. (8.22) becomes

$$4\eta_o^6(1-2\eta_o)^3 - 16Q_1^2\eta_o^6 - 4\eta Q_1^2\eta_o^3(1-2\eta_o)^3 + 8Q_1^4\eta_o^3 + Q_1^4(1-2\eta_o)^3 = 0 \qquad (8.41)$$

The condition for overmixing is $\partial Q_1^2/\partial\eta_o = 0$. Differentiating Eq. (8.41) we get

$$-12\eta_o^6(1-2\eta_o)^2 + 12Q_1^2\eta_o^3(1-2\eta_o)^2 - 3Q_1^4(1-2\eta_o)^2 + 12\eta_o^5(1-2\eta_o)^3$$

$$-48Q_1^2\eta_o^5 + 12Q_1^4\eta_o^2 - 6Q_1^2\eta_o^2(1-2\eta_o)^3 = 0 \qquad (8.42)$$

The two equations (8.41) and (8.42) determine the problem and the relevant solution is

$$\eta_o = \tfrac{1}{4}, \quad Q_1^2 = \frac{1}{64} \qquad (8.43)$$

In dimensional terms, the outgoing fluid has a thickness of H/2 and a flux

$$q_1 = \frac{HW(H\Delta b_o)^{\frac{1}{2}}}{8} \qquad (8.44)$$

A laboratory model was constructed to study a three-layer circulation. A long channel of width W_o was used as shown in cross-section and in plan view in Fig. 8.4. The opening between the harbor and the outside region has a uniform width W. The outflowing fluid has a vertical thickness aH far downstream. Attention was confined to the case of fluids of equal depth so that $\beta = \frac{1}{2}$.

Let us first consider the steady-state theory for an infinitely long channel. A portion of the problem is identical to that considered above and we are led to equations identical to Eqs. (8.41) and (8.42). The solution is again $\eta_o = \frac{1}{4}$, $Q_1^2 = 1/64$. To obtain an equation for a, we use the Bernoulli equations for the outflowing fluid and for either the upper or lower fluid. These are

$$g\Delta H + \frac{q_o^2}{2W^2\eta_o^2H^2} = \frac{2q_o^2}{W_o^2H^2(1-a)^2} \qquad (8.45)$$

$$\frac{\Delta b_o}{2}(1-\eta_o)H + g\Delta H + \frac{4q_o^2}{2W^2(1-2\eta_o)^2H^2} = \frac{\Delta b_o}{4}H(1+a) + \frac{4q_o^2}{2W_o^2a^2H^2} \qquad (8.46)$$

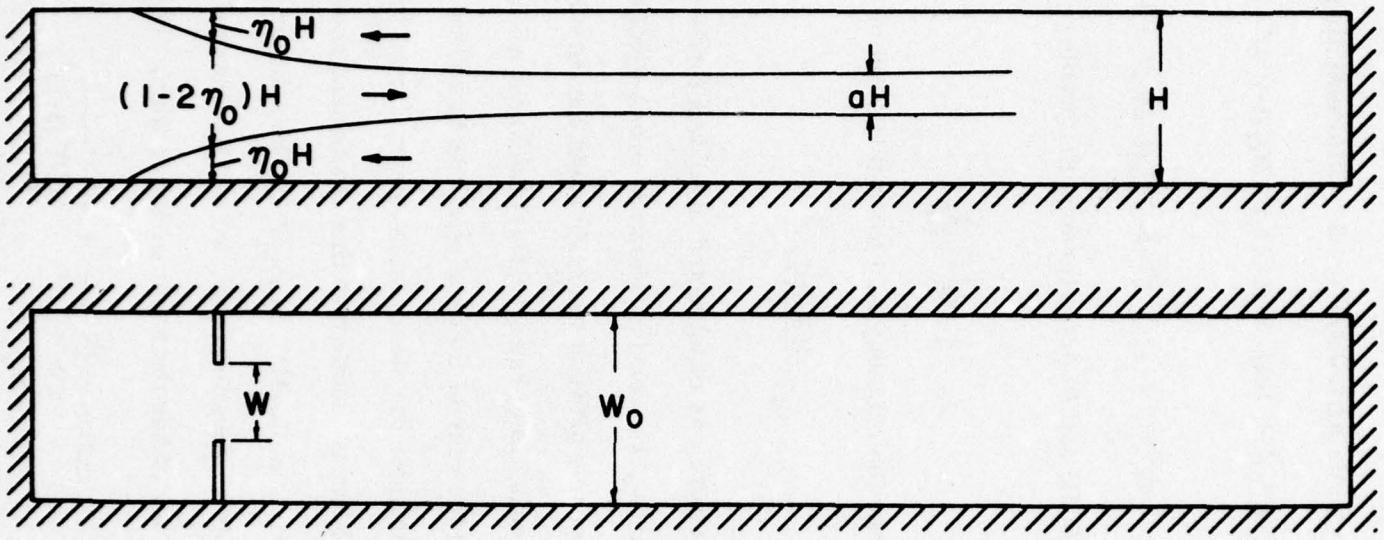

Fig. 8.4 Experiment. Axial and plan view.

Eliminating $g\Delta H$ between these two equations, we get

$$\frac{1}{4} - \frac{\eta_o}{2} - \frac{a}{4} + \frac{Q_1^2}{2(1-a)^2}\,\frac{W^2}{W_o^2} - \frac{Q_1^2}{8\eta_b^2} + \frac{Q_1^2}{2(1-2\eta_b)^2} - \frac{Q_1^2}{2a^2}\,\frac{W^2}{W_o^2} = 0 \qquad (8.47)$$

Using $\eta_o = 1/4$, $Q_1^2 = 1/64$ and imposing the condition $a \approx 0$, $W/W_o \approx 0$, we obtain

$$a = \tfrac{1}{2}\left[1-\left(1-\frac{W}{W_o}\right)^{\frac{1}{2}}\right] \qquad (8.48)$$

A graph of this relationship is shown in Fig. 8.5.

The experiment was conducted by putting a two-layer system of equal depths in the channel and then using several egg-beaters to mix the fluid in the harbor. The fluid in the harbor was thoroughly mixed in a few seconds and the middle layer began to move down the channel in a surge. Evidently a quasi-steady state resulted in the vicinity of the mouth of the harbor before the surge was able to reach the other end of the channel and reflect. The middle layer was unfortunately still quite turbulent near the mouth and for some distance along the channel, but to the extent that observation of its thickness was possible, it was close to H/2 at the mouth in accordance with the theory and as evidenced by the photograph of Fig. 8.6. The thickness ratio a was considerably larger than Eq. (8.48) indicates, probably because of the presence of a "drowned" hydraulic jump downstream.

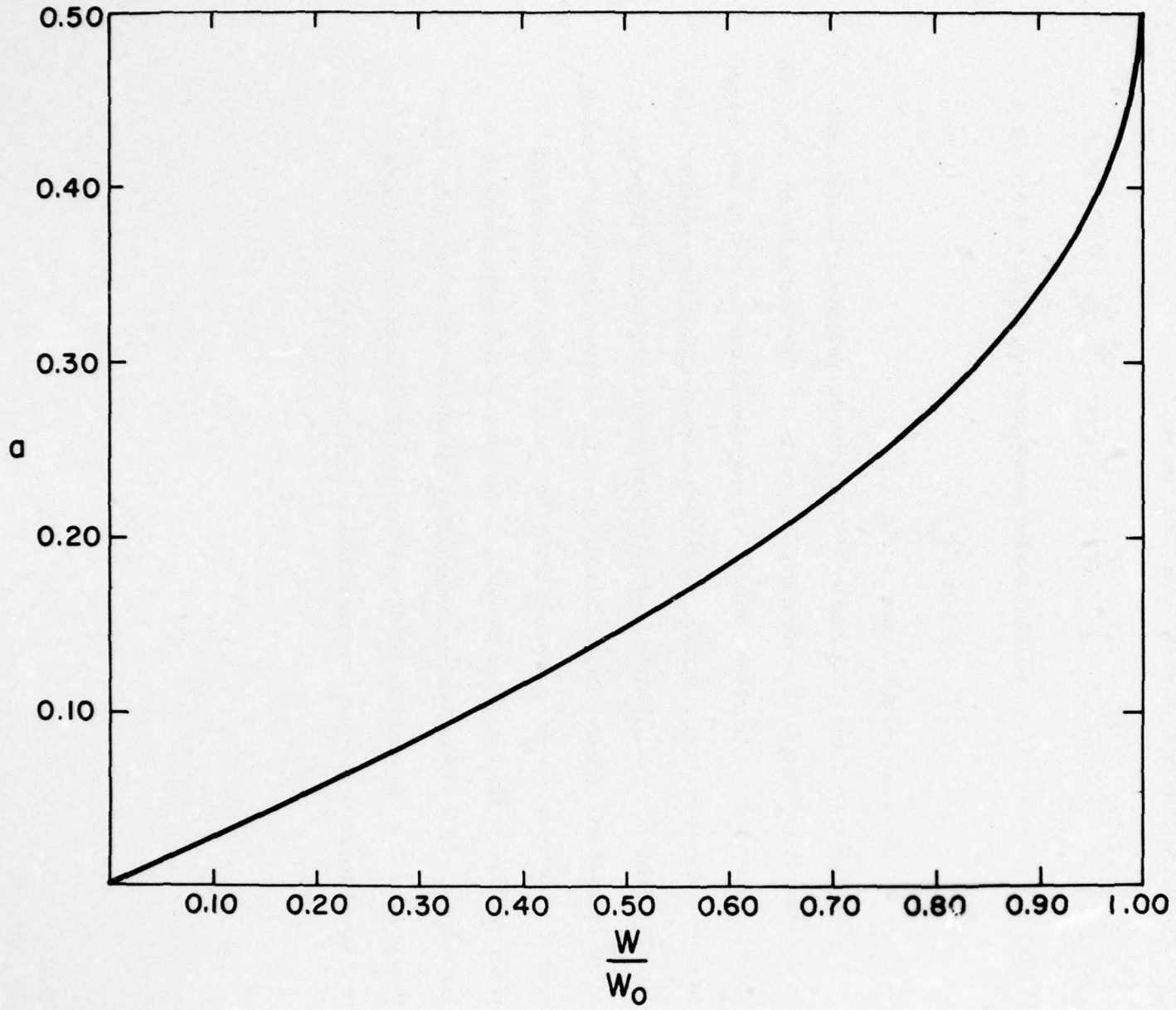

Fig. 8.5 Graph of Eq. 8.48.

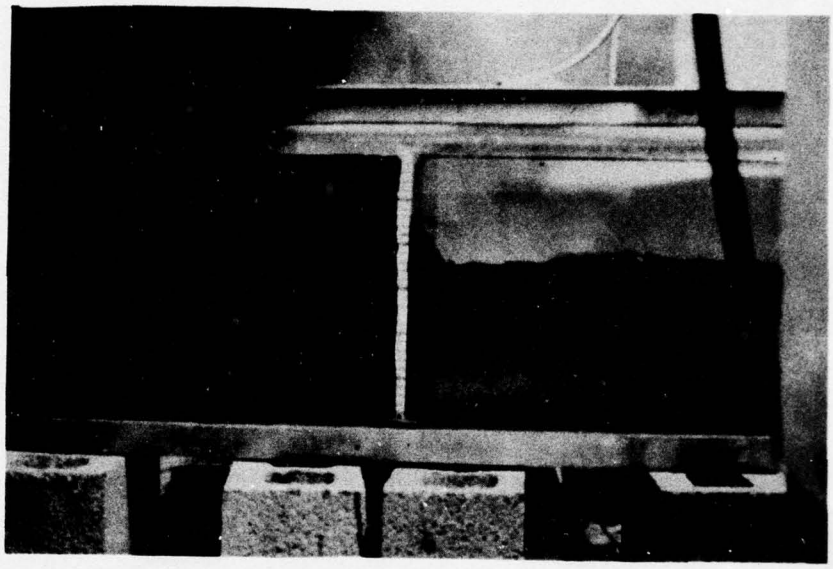

Fig. 8.6 Flow from laboratory model of an estuary.

AD-A034 119 JOHNS HOPKINS UNIV BALTIMORE MD F/G 8/8
LECTURES ON ESTUARINE CIRCULATIONS AND MASS DISTRIBUTIONS.(U)
DEC 76 R R LONG
UNCLASSIFIED TR-9-SER-C NL

2 OF 2
ADA034119

END
DATE
FILMED
2 - 77

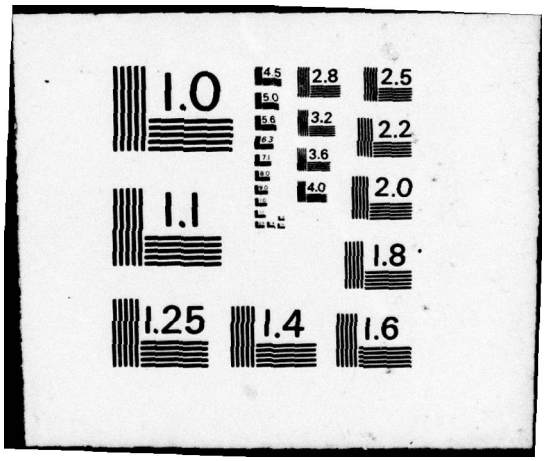
1.0
1.1
1.25
1.4
1.6
1.8
2.0
2.2
2.5
2.8
3.2
3.6
4.0
4.5
5.0
5.6

REFERENCES

Assaf, G., Anati, D.A., and Siegenthaler, U., 1977 Overmixing in sea straits: Laboratory models. (To appear in J. Fluid Mech.)

Assaf, G. and Hecht, A., 1974 Sea straits: a dynamical model. Deep Sea Res., 21, 947-958.

Baines, W.D., 1975 Entrainment by a plume or jet at a density interface. J. Fluid Mech., 68, 309-320.

Binney, A.M., 1972 Hugoniot's method applied to stratified flow through a constriction. J. Mech. Eng. Sci., 14, 72-73.

Bouvard, M. and Dumas, H., 1967 Application de la méthode de fil chaud à la mesure de la turbulence dans l'eau. Houille Blanche, 22, 257-723.

Bowden, K.F., Fairbairn, L.A., and Hughes, P., 1959 The distribution of shearing stresses in a tidal current. Geophys. J. Roy. Astron. Soc., 2, 288-305.

Brogmus, W., 1952 Eine Revision des Wasserhaushaltes der Ostsee. Kieler Meeres-forsch. 9, No. 1.

Brush, L.M., 1970 Artificial mixing of stratified fluids formed by salt and heat in a laboratory reservoir. N.J. Water Resources Res. Inst. Res. Project B-024.

Businger, J.A., Wyngaard, J.C., Izumi, Y., and Bradley, E.F., 1971 Flux-profile relationships in the atmospheric surface layer. J. Atmos. Sci., 28, 181-189.

Crapper, P.F., 1973 An experimental study of mixing across density interfaces. Ph.D. thesis, University of Cambridge.

Crapper, P.F. and Linden, P.F., 1974 The structure of turbulent density interfaces. J. Fluid Mech., 65, 45-63.

Cromwell, T., 1960 Pycnoclines created by mixing in an aquarium tank. J. Mar. Res. 18, 73-82.

Fonselius, S.H., 1962 Hydrography of the Baltic deep basins. Fishery Bd. of Sweden, Series Hydrography, No. 13, 41 pp.

Fonselius, S.H., 1967 Hydrography of the Baltic deep basins, II. Fishery Bd. of Sweden, Series Hydrography, No. 20, 31 pp.

Fonselius, S.H., 1969 Hydrography of the Baltic deep basins III. Fishery Bd. of Sweden, Series Hydrography, No. 23, 97 pp.

Gade, H., 1970 Hydrographic investigations in the Oslofjord. A study of water circulations and exchange processes, Vol. I, II and III. Geophys. Inst. Univ. of Bergen, Norway.

Hachey, H. B., 1934 Movements resulting from mixing of stratified waters. J. Biol. Bd. Canada, 1, 133-143.

Hansen, D. V., and Rattray, M., Jr., 1972 Estuarine circulation induced by diffusion. J. Mar. Res., 30, 281-294.

Hinze, J. O., 1959 Turbulence, McGraw-Hill.

Kantha, L. H., 1975 Turbulent Entrainment at the Density Interface of a Two-Layer Stably Stratified Fluid System. Tech. Rep. 75-1, Geophysical Fluid Dynamics Laboratory, The Johns Hopkins University.

Kato, H., and Phillips, O. M., 1969 On the penetration of a turbulent layer into a stratified fluid. J. Fluid Mech., 37, 643-655.

Keulegan, G. H., 1949 Interfacial instability and mixing in stratified flows. J. Res. Nat. Bur. Standards, 43, 487-500.

Kullenberg, G., 1955 Restriction of the underflow in a transition. Tellus 7, 215-217.

Linden, P. F., 1973 The interaction of a vortex ring with a sharp density interface: a model for turbulent entrainment. J. Fluid Mech., 60, 467-480.

_____, 1975 The deepening of a mixed layer in a stratified fluid. J. Fluid Mech., 71, 385-405.

Long, R. R., 1970 A theory of turbulence in stratified fluids. J. Fluid Mech., 42, 349-365.

_____, 1972 Turbulence from breaking of internal gravity waves. Rapports et Procès-Verbaux, 162, 7-18.

_____, 1973 Some properties of horizontally homogeneous, statistically steady turbulence in a stratified fluid. Boundary-Layer Met. 5, 139-157.

_____, 1975a The influence of shear on mixing across density interfaces. J. Fluid Mech. 70, 305-320.

_____, 1975b Circulations and density distributions in a deep, strongly stratified, two-layer estuary. J. Fluid Mech., 71, 529-540.

_____, 1976 Mass and salt transfers and halocline depths in an estuary. Tellus, 28, 460-472.

Moore, M. J. and Long, R. R., 1971 An experimental investigation of turbulent stratified shearing flow. J. Fluid Mech., 49, 635-655.

Pickard, G. L. and Rodgers, K., 1959 Current measurement in Knight Inlet, British Columbia. Fish. Res. Bd. Can. 16, 635-678.

Pritchard, D. W., 1956 The dynamic structure of a coastal plain estuary. J. Mar. Res. 15, 33-42.

_____, 1965 Lectures on Estuarine Oceanography. Chesapeake Bay Institute, The Johns Hopkins University, Baltimore, Md.

_____, 1967 What is an estuary: physical viewpoint. Estuaries, 3-5. AAAS.

Rouse, H. and Dodu, J., 1955 Turbulent diffusion across a density discontinuity. Houille Blanche 10, 405-410.

Rydberg, L, 1975 Hydrographic observations in the Gullmarfjord during April, 1973. Report No. 10, Göteborgs Universitet Oceanografiska Institutionen, Sweden.

Stigebrandt, A., 1976 Vertical diffusion driven by internal waves in a sill fjord. J. Physical Oceanography, 6, 486-495.

Stommel, H., 1951 Recent developments in the study of tidal estuaries. WHOI Tech. Rep., Ref. No. 51-33.

Stommel, H., and Farmer, H. G., 1952 Abrupt change in width in a two-layer open channel flow. J. Mar. Res., 11, 205-214.

_____, 1953 Control of salinity in an estuary by a transition. J. Mar. Res., 12, 13-20.

Stroup, E. D., Pritchard, D. W., and Carpenter, J. H., 1961 Final Report Baltimore Harbor Study. Tech. Rep. 26, Chesapeake Bay Institute, The Johns Hopkins University.

Tennekes, H. and Lumley, J. L., 1972 A First Course in Turbulence. The MIT Press.

Thompson, S. M. and Turner, J. S., 1975 Mixing across an interface due to turbulence generated by an oscillating grid. J. Fluid Mech., 67, 349-368.

Thorpe, S. A., 1973 Turbulence in stably stratified fluids: a review of laboratory experiments. Boundary-Layer Met., 5, 95-119.

Tully, J. P., 1949 Oceanography and prediction of pulp mill pollution in Alberni Inlet. Bull. Fish. Res. Bd. Can., 83, 1-169.

Turner, J. S., 1968 The influence of molecular diffusivity on turbulent entrainment across a density interface. J. Fluid Mech., 33, 639-656.

Turner, J. S., 1973 Buoyancy Effects in Fluids, Chap. 9. Cambridge University Press.

Welander, P., 1974 Two-layer exchange in an estuary basin with special reference to the Baltic Sea. J. Phys. Oceanogr. 4, 542-556.

Wolanski, E. J., 1972 Turbulent entrainment across stable density-stratified liquids and suspensions. Ph. D. thesis, The Johns Hopkins University.

Wolanski, E. J., and Brush, L. M., 1975 Turbulent entrainment across stable density step structures. Tellus, 27, 259-268.

Wu, J., 1973 Wind-induced turbulent entrainment across a stable density interface. J. Fluid Mech. 61, 275-287.